

**SAKARYA UNIVERSITY  
INSTITUTE OF SCIENCE AND TECHNOLOGY**

**EFFECT OF MECHANICAL ANCHORAGE IN HEAT  
TREATED BEAMS RETROFITTED BY CFRP PLATE**

**M.Sc. THESIS**

**Abdul Majeed QARIZADA**

**Department : CIVIL ENGINEERING**  
**Field of Science : CONSTRUCTION**  
**Supervisor : Assist. Prof. Dr. Yusuf SÜMER**

**October 2017**

SAKARYA UNIVERSITY  
INSTITUTE OF SCIENCE AND TECHNOLOGY

**EFFECT OF MECHANICAL ANCHORAGE IN HEAT  
TREATED BEAMS RETROFITTED BY CFRP PLATE**

**M.Sc. THESIS**

**Abdul Majeed QARIZADA**

**Department : CIVIL ENGINEERING**  
**Field of Science : CONSTRUCTION**  
**Supervisor : Assistant Prof. Dr. Yusuf SÜMER**

**This thesis has been accepted unanimously by the examination committee on 26.10.2017**

**Assoc. Prof. Dr. Seval  
PINARBAŞI  
ÇUHADAROĞLU**  
.....  
**Head of Jury**

**Assist. Prof. Dr.  
Yusuf SÜMER**  
.....  
**Jury Member**

**Assist. Prof. Dr. Hakan  
ASLAN**  
.....  
**Jury Member**

## DECLARATION

I declare that all the data in this thesis was obtained by myself in academic rules, all visual and written information and results were presented in accordance with academic and ethical rules, there is no distortion in the presented data, in case of utilizing other people's works they were refereed properly to scientific norms, the data presented in this thesis has not been used in any other thesis in this university or in any other university.

Abdul Majeed QARIZADA



26.10.2017

## **ACKNOWLEDGMENT**

This note is to thank all those special ones who have continuously maintained their support during my post graduate studies over the last years. Initially, I am infinitely grateful to my advisor, Assist. Prof. Dr. Yusuf SÜMER, who has agreed to perform as my advisor in the accomplishment of this subject and appreciate his efforts and feedback; especially during my thesis period, a very special thank is due to Assist. Prof. Dr. Emine Aydin for her guidance and support during the experimental and numerical studies. I am truly grateful for all of her assistance due to that I steered this process. It was not possible to accomplish this thesis without her assistance and support!

A note of thanks is also due to all International students studying in Turkey and Turkish students with whom I have unforgettable memorial moments, definitely, I will miss them all. I also wish to thank all those Afghan students and friends who have supported me in any aspect and never let me feel alone far from my country. In addition, this thesis would not have been perfectly possible without Okan Bakbak and Yeşim Tümsek to whom I am grateful for the language review and translation support. Further acknowledgment and thanks are due to Turkish Scholarship Committee for providing the full master studies package scholarship and accommodation, both of which were much more economically supportive.

Finally, but most importantly, I am grateful to express my special gratitude to my family, especially my elder brother Mohammad Bilal Qarizada, who has encouraged and continuously supported me during my education and I am pleased for their enthusiasm due to which I gained my goal. Meanwhile, I praise Allah for blessing me with a baby boy who colored my life with cheers. It is to conclude that this thesis was not possible to be accomplished without the support of all these tremendous and kind people!

## TABLE OF CONTENTS

ACKNOWLEDGMENT .....	i
LIST OF SYMBOLS AND ABBREVIATIONS .....	v
LIST OF FIGURES .....	vi
LIST OF TABLES .....	ix
SUMMARY .....	x
ÖZET .....	xi
CHAPTER 1.	
INTRODUCTION .....	1
1.1. Background .....	1
1.2. Objective .....	4
1.3. Scope .....	5
CHAPTER 2.	
LITERATURE .....	8
2.1. Flexure test .....	8
2.2. Heat treatment .....	10
2.3. FRP as a strengthening material .....	13
CHAPTER 3.	
MATERIAL AND ARRANGEMENT .....	21
3.1. Properties of materials .....	21
3.1.1. Steel .....	21
3.1.2. CFRP .....	24
3.1.3. Adhesive epoxy .....	27

3.2. Arrangement of lab works .....	28
3.2.1. Beam cross section .....	29
3.2.2. Preparation of steel plates .....	31
3.2.3. Creating of local deformation .....	32
3.2.4. Mechanical heat treatment .....	33
3.2.5. Drilling holes in flanges.....	34
3.2.6. Installation of CFRP .....	34
3.3. Test setup .....	36
3.3.1. Universal testing machine (High capacity).....	36
3.3.2. Universal testing machine (Low capacity).....	37
3.3.3. Drilling machine.....	38
CHAPTER 4.	
LAB STUDIES.....	39
4.1. Initial experiment.....	40
4.1.1. Reference and heat-treated IPE 80 beams.....	40
4.1.2. CFRP retrofitted IPE 80 beams .....	41
4.2. Choosing type of anchorage .....	44
4.3. Final experiment .....	47
4.3.1. Reference IPE 80 beam.....	47
4.3.2. CFRP and mechanically retrofitted IPE 80 beams .....	48
CHAPTER 5.	
VERIFICATION OF FEM MODAL .....	52
5.1. Modeling of materials .....	53
5.1.1. Steel .....	53
5.1.2. Adhesive material .....	55
5.1.3. CFRP.....	57
5.2. Types of FEM elements.....	58
5.2.1. S4R element type.....	59
5.2.1. COH3D8 element type.....	60

5.3. Boundary conditions .....	61
5.4. Geometry imperfection .....	61
5.5. Mesh.....	63
5.6. Fasteners.....	64
5.7. Model verification.....	64
CHAPTER 6.	
PARAMETRIC STUDY .....	69
6.1. FEM experimental results .....	71
CHAPTER 7.	
RESULTS AND RECOMMENDATIONS .....	80
REFERENCES .....	83
RESUME.....	88

## LIST OF SYMBOLS AND ABBREVIATIONS

AFRP	: Aramid Fiber Reinforced Polymer
ASTM	: America Society of Testing Materials
CFRP	: Carbon Fiber Reinforced Polymer
E	: Elastic modulus
FEM	: Finite Element Method
FHWA	: Federal Highway Administration
FRP	: Fiber Reinforced Polymer
GFRP	: Glass Fiber Reinforced Polymer
GPa	: Giga Pascal
$K_{nn}$	: Rigidity matrix in normal direction
$K_{ss}$	: Rigidity matrix in 1 <sup>st</sup> shear direction
$K_{tt}$	: Rigidity matrix in 2 <sup>nd</sup> shear direction
MPa	: Mega Pascal
$t_n$	: Nominal traction stress, normal direction
$t_n^o$	: Nominal stress in the damage initiation stage, normal direction
$t_s$	: Nominal traction stress, 1 <sup>st</sup> shear direction
$t_s^o$	: Nominal stress in the damage initiation stage, 1 <sup>st</sup> shear direction
$t_t$	: Nominal traction stress, 2 <sup>nd</sup> shear direction
$t_t^o$	: Nominal stress in the damage initiation stage, 2 <sup>nd</sup> shear direction
UTM	: Universal Testing Machine
$\sigma_y$	: Normal yielding stress of structural steel
$\mu$	: Poisson's ratio
$\epsilon_n$	: Nominal strain in the damage initiation stage, normal direction
$\epsilon_s$	: Nominal strain in the initiation stage, 1 <sup>st</sup> shear direction damage
$\epsilon_t$	: Nominal strain in initiation stage, 2 <sup>nd</sup> shear direction the damage



## LIST OF FIGURES

Figure 2.1. Types of flexure test.....	9
Figure 2.2. Bending test diagram [14]. .....	10
Figure 2.3. Heat treatment of steel girders [7].....	11
Figure 2.4. Heat treatment of compression plates [15].....	12
Figure 2.5. Heat treatment of fixed plates [4]. .....	12
Figure 2.6. Heat treatment of rectangular hollow steel column [17].....	13
Figure 2.7. HM-CFRP strengthened composite I girder [32].....	15
Figure 2.8. Experimental specimen beam geometry [37]. .....	17
Figure 2.9. Cross section configuration of specimen and test set up [42]. .....	19
Figure 2.10. Experimental set-up [43]. .....	20
Figure 3.1. Standard dimensions of tensile test specimen. ....	22
Figure 3.2. Tensile test.....	22
Figure 3.3. Tensile test of reference specimen. ....	23
Figure 3.4. Tensile test of heat-treated specimen. ....	23
Figure 3.5. Stress and strain diagram for reference and heat-treated specimens. ..	23
Figure 3.6. Typical tabbed CFRP tensile specimen [50]. .....	25
Figure 3.7. CFRP specimen for tensile test.....	26
Figure 3.8. Behavior of CFRP specimen after the tensile test. ....	26
Figure 3.9. Stress and strain diagram for CFRP tensile test specimen. ....	27
Figure 3.10. Admixture of epoxy [4]. .....	28
Figure 3.11. IPE 80. ....	29
Figure 3.12. IPE 80 steel cross section. ....	30
Figure 3.13. Steel plate and tying options.....	31
Figure 3.14. Drilled holes in steel plate and CFRP and bolt anchorage. ....	32
Figure 3.15. Creating of local deformation. ....	32
Figure 3.16. Heat treating and straightening of specimens.....	33

Figure 3.17. Straightened and heat-treated shape of test specimens. ....	34
Figure 3.18. Drilling procedure for steel beam. ....	34
Figure 3.19. Applying epoxy & CFRP on the face of specimens. ....	35
Figure 3.20. Employing bolts & clamping the specimens. ....	35
Figure 3.21. The specimens ready for lab experiment.....	36
Figure 3.22. AŞLAN UTM machine [52]. ....	37
Figure 3.23. AG-IC Table-Top type UTM [53]. ....	38
Figure 3.24. Optimum B20 drilling machine [54]. ....	38
Figure 4.1. Force-displacement graph for IPE 80 RB and HT specimens.....	41
Figure 4.2. IPE 80 Reference beam before and after the test.....	41
Figure 4.3. Force-displacement graph for IPE 80 RB & carbon retrofitted.....	43
Figure 4.4. Types of anchorage. ....	44
Figure 4.5. CFRP retrofitted steel plates under four-point bending test.....	46
Figure 4.6. Force-displacement graph for steel plates specimens. ....	46
Figure 4.7. Reference beam before and after the test. ....	48
Figure 4.8. Force-displacement graph for reference beam.....	48
Figure 4.9. Retrofitted beams under three-point bending test.....	49
Figure 4.10. Force-displacement graph of reference and retrofitted beams.....	51
Figure 5.1. Conventional and true stress and strain diagrams of steel [57]. ....	54
Figure 5.2. Ideal elastic-plastic behavior of materials. ....	55
Figure 5.3. FEM suggested model. ....	56
Figure 5.4. Fully integrated linear and quadratic elements [56]. ....	58
Figure 5.5. Reduced integrated linear and quadratic elements [56]. ....	59
Figure 5.6. S4R element type [56]. ....	59
Figure 5.7. Naming convention of cohesive elements [56]. ....	60
Figure 5.8. COH3D8 element type [56]. ....	60
Figure 5.9. Boundary conditions of the model. ....	61
Figure 5.10. Buckling eigen value modes for imperfection [56]. ....	62
Figure 5.11. Meshing sensitivity of a model. ....	63
Figure 5.12. Mesh-independent point fasteners [56]. ....	64
Figure 5.13. FEM IPE 80 RB. ....	65
Figure 5.14. FEM IPE 80 HTC. ....	65

Figure 5.15. FEM IPE 80 HTCBr.....	66
Figure 5.16. Force and displacement diagram (RB IPE 80).....	66
Figure 5.17. Force and displacement diagram (HTCr IPE 80).....	67
Figure 5.18. Force and displacement diagram (HTCbr IPE 80).....	67
Figure 6.1. Force and displacement diagram (MODEL 1).....	71
Figure 6.2. Force and displacement diagram (MODEL 2).....	72
Figure 6.3. Force and displacement diagram (MODEL 3).....	72
Figure 6.4. Force and displacement diagram (MODEL 4).....	73
Figure 6.5. Force and displacement diagram (MODEL 5).....	73
Figure 6.6. Force and displacement diagram (MODEL 6).....	74
Figure 6.7. Force and displacement diagram (MODEL 7).....	74
Figure 6.8. Force and displacement diagram (MODEL 8).....	75
Figure 6.9. Force and displacement diagram (MODEL 9).....	75
Figure 6.10. Force and displacement diagram (MODEL 10).....	76
Figure 6.11. Force and displacement diagram (MODEL 11).....	76
Figure 6.12. Force and displacement diagram (MODEL 12).....	77
Figure 6.13. Effect of mechanical anchorage in compact and non-compact sections. ... .....	79

## LIST OF TABLES

Table 2.1. Properties of materials [10].....	14
Table 3.1. Mechanical properties of reference and heat-treated specimens .....	24
Table 3.2. Dimensions of CFRP tensile test specimens.....	25
Table 3.3. Mechanical properties CFRP .....	27
Table 3.4. Properties adhesive epoxy .....	28
Table 3.5. Dimensions of IPE 80 section.....	30
Table 3.6. Geometrical properties of IPE 80 section.....	30
Table 4.1. Arrangement of CFRP plates .....	42
Table 4.2. Arrangement of steel shell plates .....	45
Table 4.3. Arrangement of CFRP plates .....	49
Table 4.4. Lab experimental results.....	51
Table 5.1. Mechanical property of steel for FEM models .....	55
Table 5.2. Properties of cohesive elements.....	57
Table 5.3. Properties of CFRP elements .....	57
Table 6.1. Parameters of the specimens for parametric study.....	70
Table 6.2. Comparison of FEM reference beams against mechanically retrofitted beams .....	77

## **SUMMARY**

Keywords: Locally damaged beams, Heat treatment, Repair, CFRP, Bolt Anchorage

Locally deformed beams and girders can be temporarily repaired by heat treatment but this practice causes decrease in the load capacities of the members. Besides, fiber reinforced polymer strips can be used to gain permanent retrofitting solution for the damaged members. In this study initially, the behavior of a heat treated beam with IPE-80 cross section strengthened by Carbon Fiber Reinforced Polymer (CFRP) plates bonded with epoxy is studied. This repair technique is observed to causes a significant increase in load capacity but it is also being recognized that epoxy scatters earlier, which causes premature failure of the CFRP plate.

This study suggests the implementation of anchorages through bolts or CFRP fabrics along with epoxy bonding while placing CFRP plates to retrofit the heat treated elements. Preliminary experiments conducted on plates specimen show that using anchorage by employing bolt lead to large increase compared to using anchorage made by CFRP fabric only. Then, scaled steel beams with IPE80 sections are selected and they are subjected to the three-point bending test.

In the final stage of the study, finite element models are constructed to examine the effects of bolt anchorage on larger specimens. After verification of the finite element model, to obtain the most effective specimen a parametric study is carried out. The experimental and FEM studies determines that additional anchorage provides better bonding and causes the elements to resist larger loads. The practice medium span non-compact section with the highest web slenderness ratio has mostly increased the load capacity of its related Reference beam (35.6 %) compared to its other counterparts.

# ÇELİK KİRİŞLERİN ONARILMASINDA KULLANILAN CFRP LEVHALARIN ANKRAJLARININ İNCELENMESİ

## ÖZET

Anahtar Kelimeler: Hasarlı çelik kirişler, Isıl işlem, Güçlendirme, CFRP, Bulonlu ankraj

Yerel burkulma nedeniyle hasar görmüş çelik kirişler ısıl işlemle geçici olarak onarılabilir. Ancak bu uygulama elemanın yük kapasitesinde azalmaya neden olmaktadır. Isıl işlemi ek olarak, elyaf takviyeli polimer şeritler hasar görmüş yapı elemanlarının iyileştirilmesi için kullanılmaktadır. Bu çalışmanın ilk aşamasında, ısıl işlem görmüş ve Karbon Fiber Takviyeli Polimer (CFRP) levhalarla güçlendirilmiş IPE-80 enkesitli bir kiriş yük altındaki deneysel olarak araştırılmıştır. Deneysel çalışmanın sonucunda CFRP levhalarla yapılan güçlendirmenin yük kapasitesinde belirgin bir artışa neden olduğu, ancak epoksinin erken sıyırılması nedeniyle CFRP'nin dayanımından yeteri kadar yararlanılamadığı gözlenmiştir.

Bu amaçla, öncelikle CFRP kumaşların epoksi yardımıyla ısıl işlem görmüş çelik kirişe ankrajı, ve sonraki aşamada ise CFRP malzemenin bulonlar kullanılarak daha kalıcı şekilde hasarlı bölgeye ankre edebilmesiyle çelik kirişlerin dayanımları deneysel olarak araştırılmıştır. Çelik plakalara uygulanan eğilme deneylerinde bulon kullanılarak yapılan güçlendirme ile CFRP kumaştan yapılan ankraj kullanılarak yapılan güçlendirme karşılaştırıldığında, bulonlu ankraj uygulamasının daha iyi sonuçlar verdiği görülmüştür. Deneysel çalışmaların üçüncü aşamasında ölçeklendirilmiş IPE80 enkesitli çelik kirişlere üç nokta eğilme deneyi uygulanmıştır. Gerçek boyutlu kirişlerin analizi için deneysel sonuçları sonlu elemanlar modeliyle doğrulandıktan sonra yüksel narinlikli gerçek boyutlu kirişlerde de 35,6'ya dayanımı arttırdığı görülmüştür.

# CHAPTER 1. INTRODUCTION

## 1.1. Background

Buckling occurs out of the plane of the transverse load, if the torsional and lateral stiffness of the beam is relatively smaller compared to the stiffness of the beam in the plane of loading or its lateral restraints are inadequate.

A perfectly straight and elastic beam does not face out of plane deformations until it experiences a critical value of the applied load, while at this stage lateral deflection and twisting occurs in the beam, which causes buckling [1].

These external loads may be applied to the structure due to earthquake, wind, fire, fatigue and etc. As the critical load value is being reached, a hardly noticeable change of deformation happens in the geometry of the steel member, which causes the member to lose its ability in order to bear the loads, eventually, at such a stage, the structure is considered to have deformed.

The deformation of structural elements, also known as structural instability, after losing its load carrying capacity results reduction of stiffness or strength loss in a section, which could be restrained by repairing procedures in emergency conditions for temporary uses. These repairing procedures are performed to re-establish the resistance and serviceability of the structure [2].

The following types of methods are commonly employed to repair the defects:

- a. Flame straightening
- b. Hot mechanical straightening

- c. Cold mechanical straightening
- d. Welding
- e. Bolting
- f. Partial replacement
- g. Full replacement

Steel beam sections can be repaired either by the flame (heat) straightening method or by hot mechanical straightening, but flame straightening is known as a preferable method to be considered for all primary tension members instead of hot mechanical straightening, where ever feasible. Hot mechanical straightening is an appropriate method to strengthen all primary compression members or secondary members. To carry out this method, the operators should have sufficient skill to repair the members in such a manner that should be free of wrinkles, bulges, cracks, and poor alignment.

By the heat treatment at high temperatures the tensile stress, yield stress and elastic modulus of steel reduce significantly. According to the tests conducted by FHWA (Federal Highway Administration) for the determination of the damages and repairs on steel due to repetitive cycles, it is found that yield stress increases significantly after two or more repair cycles.

The increase of the tensile strength at the apex of the vee (heat pattern) was also observed which is about half that of the yield stress. In addition, there is a significant decrease in ductility at the at the apex region. It is suggested by FHWA that no more than two damage or repair cycles should be carried out by heat strengthening, since gap declines between yield stress and normal tensile strength.

Repeated heat straightening was performed by Although Alberta Transportation on several damaged structures which did not contain any detrimental effect. It is noticed that multiple heat straightening increases the risk of cracking, thus they recommend to cautiously carry out the multiple heat straightening by qualified personnel under



the strict supervision, whereas the proposed heat straightening solution for damage restoration was found so cost-effective [2].

As per the studies and researches, it shows that repair of steel structural elements can be fixed by heat treatment but it causes decrease in their strength. In addition, Aydin and Aktas in their research show that a decrease of 10 % can occur due to heat treatment of structural steel elements, so, therefore, it could only be considered as a temporary repair for damaged steel structures [4].

In addition to the heat treatment, in order to gain a permanent solution for the damaged structural steel elements, the Fiber Reinforced Polymer (FRP) is an effective treatment to upgrade, retrofit, and strengthen the damaged, deteriorate, or deficient concrete or steel structures. To upgrade the cracked or damaged areas, the composite strips and plates are affixed to the concrete structure by pasting adhesive, wet lay-up, or infusion of resin. To retrofit the steel structural element, the composite plates are usually attached to their flanges, which improves both the stiffness and strength of the flanges [3], [5], [6].

Application of FRP composite can result to increase [6], [10], [11]:

- a. Axial tensile capacity
- b. Flexural capacity
- c. Shear capacity
- d. Fatigue life
- e. Stiffness

In addition, FRP composite has a high elastic modulus, high strength to weight ratio, corrosion and fatigue resistance, and is significantly durable. In case; if access is not feasible to the section, the application of the FRP composite becomes highly effective. The application of the FRP composite is not time-consuming, which utilizes less time compare to the conventional repair techniques [10], [11].

Fiber-Reinforced Polymer composites consist of three main constituents, which are [6], [11]:

- a. High-strength fibers (CFRP, AFRP or GFRP)
- b. Polymeric matrix
- c. Additives

Since more than two decades in the field of structural engineering, the applications of High strength Fibers have become an increasingly significant material. It can be used both to retrofit and strengthen the existing structures or as an alternative reinforcing material (or pre-stressing material) instead of steel at the inception stage of a project.

In civil engineering, the consumption of these materials are increasingly dominant for retrofitting and its applications comprise of increasing the load capacity of old structures (such as bridges) seismic retrofitting, and repair of damaged structures. In many instances, retrofitting is popular because replacing the defective structure can greatly exceed in cost compared to its strengthening using CFRP [7].

It is also proved from various field practices that CFRP is itself a more cost effective material to strengthen concrete, steel, masonry, cast iron, and timber structures compared to its counterparts, such as Glass Fiber-Reinforced Polymer (GFRP) and Aramid Fiber-Reinforced Polymer (AFRP) [4], [7].

## **1.2. Objective**

The purpose of this study is to propose a permanent repair and retrofitting solution to the locally damaged flexural steel elements caused by disaster loads as; earthquake, fire, wind, fatigue or etc. Initially, the locally deformed or buckled elements are repaired with the heat treatment while it causes the decrease in stiffness and strength. As a solution; to gain the stiffness and load carrying capacity the Carbon Fiber Reinforced Polymer (CFRP) is proposed to be attached to the damaged elements.

As dozens of research exist on strengthening the deformed beam elements with Carbon Fiber Reinforced Polymer (CFRP), however this study proposes the implementation of bolt anchorages to the heat treated and CFRP retrofitted beam along with epoxy bonding which will cause the CFRP plates to resist much more load compare to the only epoxy bonded practice.

In the initial step, the locally deformed IPE80 Beams (EU) are taken under study at the laboratory. After proceeding the heat treatment, the effects and outputs due to the attachment of CFRP are taken under the consideration. It is revealed that this practice causes a significant increase of load capacity but it is also being observed that epoxy scatters earlier, which does not allow the CFRP to restrain for much more load. So hereafter the CFRP restrained shell plates are considered to be employed with a bolt and CFRP fabric anchorage. As result, employing bolt anchorage option has significantly better result compare to CFRP fabric anchorage and only epoxy bond. The Lab experiments finally conclude the effect of bolt anchorage implementation along with CFRP and epoxy bonding for heat the treated IPE 80 beam.

In this thesis, the nonlinear analyses of these specimens with the same parameters are performed; using Finite Element Method (FEM) ABAQUS program. Subsequently, the output results received from the program is compared with lab experiment results for verification.

After observations and verification, the most stable, effective and economic specimen is chosen among them. Thereafter the specimens are scaled to the large sizes with the constant height to width dimensions' ratio and locating the CFRP in appropriate locations for a parametric study.

### **1.3. Scope**

This study involves the permanent repair and retrofitting of deformed/damaged steel I beam after application of the heat treatment. The test specimens are respectively connected to the fixed and roller support at their ends.

The first chapter of this thesis explains the background, objective and scope of this study with an initial brief introduction of the deformed/damaged steel beam's behavior and its repairing solutions.

The second chapter consists of literature review on damaged steel beams and its behavior. Detail information is provided about the causes of beam damages and their solutions. The history, application, and specification of the FRP materials are also described by highlighting their advantages, stability and cost effectiveness.

The laboratory experiments, materials, and their applied methods are allocated in the third chapter. The procedures carried out during the lab experiments are explained step by step with their characteristics and specifications. The preparation scenes of material and specimens are depicted in the form of figures to receive a brief visual pick up of the subject. At the end of this chapter, the set-up of the specimens and the machinery used during the experiments are introduced briefly with their characteristics and advantages.

The fourth chapter describes the deformation behavior of I beam under the concentrated load carried out during the experiment. The behavior and load capacity of the deformed steel I beams are observed after the heat treatment compares to its initial load bearing state. Later on, the specimens are strengthened with CFRP for retrofitting and permanent repairing, the behavior, and effect of CFRP and anchorage are studied from the results of the experiments. All these states are figured and compared in the form of Force and displacement graphs

The fifth chapter explains the manner and characteristics of the Finite Element Program ABAQUS for modeling the steel beams. The specification of the materials used in experiments is provided with their detailing's. The output result received

from the ABABUS program is initially reviewed and eventually, their comparisons with lab experimental results are evaluated for verification.

The parametric study is carried out at the sixth chapter. After the verification of the FEM results, the most economical, stable and effective specimen is scaled with height to width dimensions' ratio and an appropriate set-up for the location and dimensions of CFRP bonding is considered. The output results from the different set-ups and different scale specimens are gathered in the form graphs for decision.

The seventh chapter describes the discussion of the results obtained from the experimental and numerical studies and summarizes main conclusions.

## **CHAPTER 2. LITERATURE**

The second chapter is consisting of literature explanation of the steel beams and its behavior. Detail information is provided about causes of beam deformation and their solutions. Different common repairing methods including heat treatment of deformed steel members are described. The history, application, and specification of the FRP materials are described by highlighting their advantages, stability and cost effectiveness. Various experiments conducted for the application and effect of FRP materials to re-strengthen steel elements are described respectively.

### **2.1. Flexure Test**

Flexure or bending tests are commonly carried out to examine the flexural rigidity/stiffness or flexural strength of all structural materials and products. This test is found much more economical compared to a tensile test and the results of them are fairly unlike. The flexure test does not measure the basic properties of material but commonly this test is considered to measure the flexural strength and flexural rigidity of the proposed material [13].

The outermost fiber of the specimen observes maximum stress at either compression or tension side, which is called as flexure strength. The flexural rigidity could be determined by a curve of strain deflection and slope of the stress. The resulted values indicate the withstanding capability of materials against flexure of bending forces [13]. The test is commonly performed by universal testing machine (UTM) or tensile testing machine (See chapter 3) with a three-point or four-point loading (See Fig. 2.1).

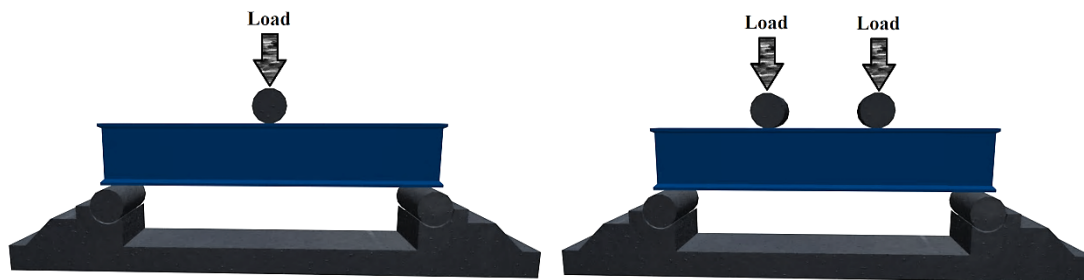


Figure 2.1. Types of flexure test.

Considering three-point bending test, the specimen is placed horizontally on two supporting pins with a set of specific distance apart and the force is applied to the top of the specimen from the above direction by the third pin with a constant rate until the specimen failure. This method causes the specimen to bent in the shape of “V”.

Four-point bending tests roughly have the same concept of appliance expect that the load from the above direction is applied to the top of the specimen by two pins with a set of appropriate distance apart and hence the specimen experiences contact at four points. In addition, in this method, unlike a three-point bending test, the specimen bends in the shape of “U”. Considering a specific location of the specimen it is ideal to perform a three-point bending test, whereas four-point bending test is perfect for considering the test of specimens with large sections. This method highlights the defect of a specimen better than a three-point bending test [13]. The below terms are the main key analyses of the bending test:

**Flexural Rigidity:** This term indicates the stiffness of the material and it determines the slope of a stress over strain curve.

**Flexural Strength:** The term is used to indicate the maximum bearing force value of a material that possesses before it is being broken or yielded. Yield indicates the status of the material where it is pushed to the state passing its recoverable deformation and the shape it once possessed could no longer be gained anymore.

**Yield Point:** The yield point indicates that the material basically “gives up” or it is the point where if bending of the material is kept continues, the increase in force will not continue; whereas, subsequently it would commence to decrease or fracture [15].

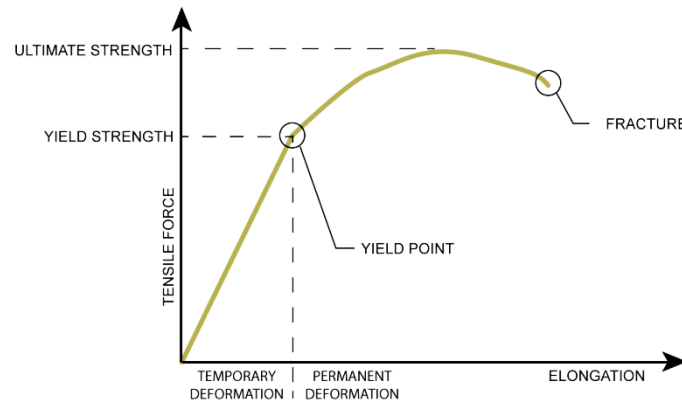


Figure 2.2. Bending test diagram [14].

## 2.2. Heat Treatment

As described earlier (Chapter 1) different types of heat treatments methods are available to repair the deformed members but the most superior and effective method, especially for all primary tension members, is the hot mechanical method. In addition, it may be used for strengthening the primary compression members.

In this process, heat is applied to all sides of a deformed member and is straightened by applying force while the member is still hot. The maximum temperature to be used during the process is restricted to 640°. The operator skill has a high influence on the result of this type of heat treatment, as the result should be free of wrinkles, cracks, bulges, and poor alignment [2].

As per national and international codes, there are some additional requirements and recommendations for the mechanical method, namely [6]:

- a. The mechanical straightening is not allowed under temperature -20°.



- b. In the last step of the operation, the maximum external forces should be kept steady for 15 minutes.
- c. Executing mechanical repair, there shall be no tolerance for cracks and defects.
- d. Torsional deformations shall be carried out after elimination of bending deformation.

As per the experimental studies, yield strength is greatly reduced after heat treatment [8].



Figure 2.3. Heat treatment of steel girders [7].

Kim and Hirohata [16] performed their experiment on steel plate compression member under axial load and have noted the buckling loads and horizontal displacements of the member. Later on, they repaired the member with heat treatment and re-applied the axial load on the member. The result received from the comparison of both experiments shows a difference of maximum load capacity which is due to a reduction in stiffness of heat treated specimens caused by stresses. Kim and Hirohata have also modeled these experiments in finite element method for verification. The applied heat treatment procedure of the specimen is shown in Fig.2.4.

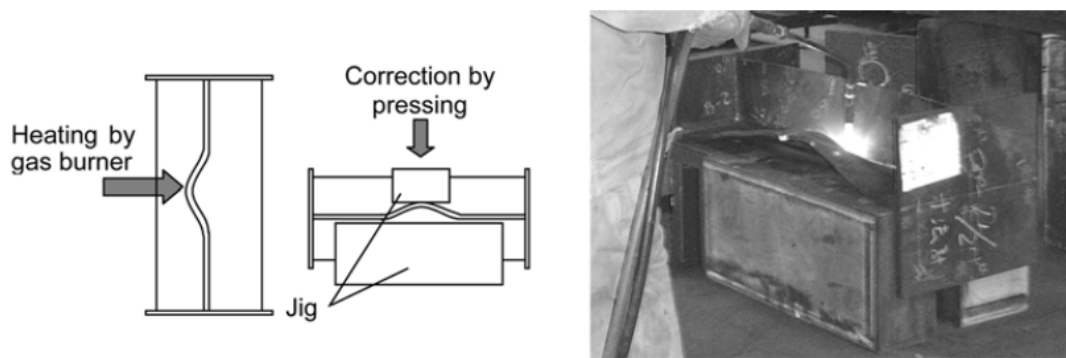


Figure 2.4. Heat treatment of compression plates [15].

Aydin and Aktas [4] as shown in the Fig (2.5) have performed a buckling test on three specimens of fixed plates under axial load. During the test, the vertical and horizontal displacements under applied loads were noted. The specimens were retaken under the same procedure and loads after heat treated. The result observed from the average of these three specimens show a significant reduction of load capacity about 20% and a reduction of 51% in stiffness of the heat treated member compare to the reference plates.

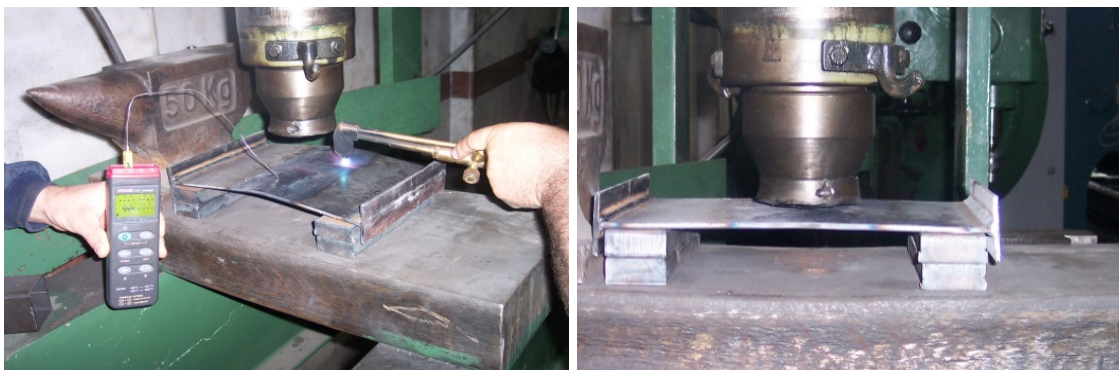


Figure 2.5. Heat treatment of fixed plates [4].

Kim and Hirohata [17] have also performed an experiment on rectangular hollow steel column at the lab; in addition, the specimen was also modeled in the finite element method for verification. Initially, a hollow steel column with the height of (H) 700 mm, the width of 400mm and with the thickness of 2 mm was heat treated

and pressed after performing the buckling test. After applying the maximum load on the heat treated member; a significant difference in the load capacity was observed.

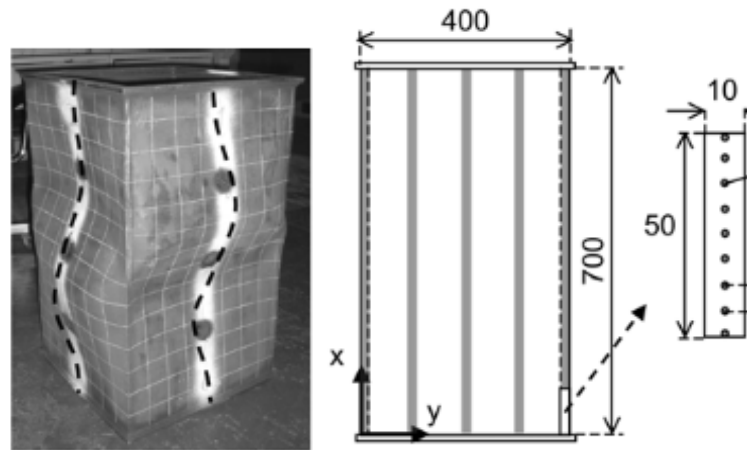


Figure 2.6. Heat treatment of rectangular hollow steel column [17].

### 2.3. FRP as a Strengthening Material

Fiber-reinforced polymers are known as a great feasible alternative to replace reinforced concrete and steel in bridges, buildings, and other civil infrastructures. [9] Since more than two decades in the field of structural engineering, the applications of high strength fibers have become an increasingly significant material. It can be used both to retrofit and strengthen the existing structures or as an alternative reinforcing material (or pre-stressing material) instead of steel at the inception stage of a project. In addition, the FRP composite has a high strength to weight ratio, high elastic modulus, corrosion resistance, fatigue resistance and being good in durability. In the case when the access to the section is difficult the FRP composite is highly effective and could be applied easily in any form. Time for FRP application is less than compared to the conventional repair techniques [6], [10], [11], [18-20].

FRP is widely used to strengthen the concrete structures. As per the latest researches performed at United States of America [21-25], United Kingdom [26-29], Japan [30]

and Swiss [31], they show a wide incensement of CFRP application for strengthening and retrofiting of steel structures.

Properties of reinforcing fibers:

There are three types of carbon fibers available which are: High Strength (HS), High Modulus (HM) and ultra-high modulus (UHM). Their thermal expansions are low but possess a high electrical conductivity. Table 2.1. shows properties of aramid, carbon and glass fibers [12].

Table 2.1. Properties of materials (Carbon fiber, Aramid fiber, and E-glass fiber) [10]

	Carbon fibers			Aramid fiber	E-glass fiber
	High-strength (HS)	High-modulus (HM)	Ultra-high modulus (HM)		
Modulus of elasticity (GPa)	230-240	295-390	440-640	125-130	70-85
Strength (MPa)	4300-4900	2740-5940	2600-4020	3200-3600	2460-2580
Strain Failure (%)	1.9-2.1	0.7-1.9	0.4-0.8	2.4	3.5
Density (Kg/m <sup>3</sup> )	1800	1730-1810	1910-2120	1390-1470	2600
Coefficient of thermal expansion (parallel to fiber), (10 <sup>-6</sup> /C)	-0.38	-0.83	-1.1	2.1	4.9

Elif Agcakoca [32] has performed lab experiments on I sectional concrete composite bridge girders. A C30 concrete slab relatively having a thickness of 50mm and 450mm wide with IPE 160 steel section were selected as the reference properties of the composite girder. Besides this three specimens having the same properties of reference beam were strengthened with HM-CFRP and later on bending test was carried on them. The result observed from the bending test shows that about 20% of load capacity increases in the strengthened composite girder compare to the reference one.



Figure 2.7. HM-CFRP strengthened composite I girder [32].

Sayyed Ahmad [33] has carried out a numerical study on local web buckling. For this purpose, CFRP laminates were applied to buckled areas for strengthening. Actually, the key advantage of this technique is set to postpone the onset of the local buckling at the web of the beam. Eventually the slender of I section will be allowed to reach its yielding flexural capacity. This study reveals that critical load significantly increases about 20-60 % due to the bonding of the CFRP laminates to the web of I-sections and it also allows the beam reaching its yield capacity.

In order to reveal the possibility of using the reinforced polymer (CFRP) epoxy laminates and to repair the composite steel bridge members, Sen and others [34] have performed an experimental investigation. Six specimens of 6.1 m long A36 steel beam with the wide flange of W8×24 performing compositely with the reinforced concrete slab respectively measured with the thickness and wideness of 0.114 m and 0.71 m were taken under lab observation. Initially, in order to simulate severe service distress, the load was applied on the specimens past yield of the tension flange. Later on CFRP laminates being 3.65 m long and 2 or 5 mm thick were bonded to the tension flange for repairing the damaged specimens, eventually, they were tested to failure. The result shows a significant increase in ultimate strength but the elastic response has modest improvement. The non-linear finite element analysis is also performed which accordingly complies with the results of Lab Experiments. The study suggests that using CFRP laminates is feasible to strengthen the steel composite members.

Chiew and others [35] have observed the de-bonding failure of the FRP laminate with the steel beams as an important consideration for fiber-reinforced polymer (FRP) steel structures. A bond failure model is proposed by them for FRP-steel structures which comprise of shear and normal strain/strain energy density components in their study. For the purpose, it is noticed that the lab and the finite element analysis (FEA), prediction of the ultimate load of the FRP retrofitted steel beam and simulation of de-bonding failure process could be successfully achieved. The predicted failure load agrees well with the measurements of Lab experiments.

Pierluigi Colombi and Carlo Poggi [36] have also accomplished the lab experiment and numerical investigation in order to determine the static behavior of steel beams reinforced with pultruded CFRP strips. The evaluation of the force transfer mechanism, the increment of the beam load carrying capacity and the bending stiffness were the main objectives of this experimental program. For the purpose different geometries of reinforcing CFRP strips are attached to the tension flanges of H shaped (traditional) steel beams. Different types of adhesive epoxies are applied in this exercise. The provided specimens are subsequently tested under three points bending operation. As a result, due to the retrofitting, it shows the increase of 11 - 65% in yielding strength. The finite element model is also presented against the experimental data for validation.

In another study, Pierluigi Colombi, Giulia Fava [37] performed fatigue test on defective steel beams and eventually suggested that Carbon Fibre Reinforced Polymers (CFRP) are more efficient under monotonic loads. The study is concluded on undertaking nine sets of cracked steel beams reinforced with CFRP strips under fatigue tests. As result observed from the fatigue crack propagation curves shows the reduction of fatigue crack growth and extension of fatigue life due to CFRP strips. It is also revealed in the Experimental results that a de-bonded area exists at the location of the crack between the strips of reinforcement and the substrate of steel. For verification, the experiment results are also compared with numerical and analytical studies.

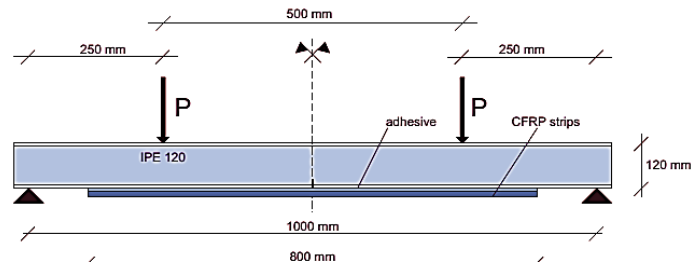


Figure 2.8. Experimental specimen beam geometry [37].

El Damaty and other [38] in their assessment have considered the application of Glass Fibre Reinforced Plastic (GFRP) sheets in order to boost the flexural capacity of steel beams. For the case study analysis, the dimensions and properties of cross section are adopted from the composite steel girder of a real bridge. A nonlinear numerical model is established with details in order to observe the former and subsequent behavior of a bridge following the installation of the GFRP sheets to the bottom flange of the composite steel girder. The assessment reveals the above-mentioned practice as an important factor that can extensively increase the capacity of a bridge.

Accord and others [39] in their study discuss the control of local buckling manifestation by using fiber-reinforced polymer composite materials in a steel section during plastic hinging. The main focus of the discussion is to carry out the technique wherein local buckling modes of a plate in an I shaped steel cross section are restricted by bracing the integral plate segments through the imposition of thin longitudinal strips which are used to enforce a nodal line along a plate element. Besides the analytical work, the study has also been investigated by simulating the nonlinear finite element models through the available commercial software called ADINA. Thus the study demonstrates that the critical load for individual steel plate elements increases in such an approach and for the same elements it helps to constrain plastic flow in order to enhance the structural ductility of the entire cross-section. In addition, it is observed that the arrangement and allocation of GFRP plates has an important impact on the results.

Panatik and Baur [40] in their study observed the effect of CFRP laminates for strengthening steel beams. For the purpose retrofitted steel beams were taken under flexure test at the lab. As a result, from their study, they have found an increase about 30% of the load capacity and 62% increase of shear capacity in the element.

A.H. Al-Saidy and others [41] examined Carbon Fiber Reinforced Polymers (CFRP) plates in their investigation in order to notice the behavior of strengthened composite steel–concrete girders. Attachment of CFRP plates to the bottom flanges of the girder has resulted in the strength achievement. In addition, CFRP plates to the web of some beams were also applied in this study. CFRP plates in two varieties that were mainly considered in this study had a different modulus of elasticity (Tensile). The team has recorded and reported the distribution of shear stress along the bond line between steel and CFRP plates. The test results received from the investigation on the steel–concrete composite girders reveal that 45% of strength and stiffness in the strengthened girders is enhanced by lightweight CFRP plates compare to the original one.

Amir Fam and others [42] in their study investigated the use of Carbon Fiber Reinforced Polymer (CFRP). The Young's modulus of the considered material was varying from 150 GPa to 400 GPa. The objective of the study was to strengthen the intact steel concrete composite girders and the rehabilitation of notched steel beams. For the purpose, the dimensions of the three large scale (6100 mm long) composite steel concrete girders were proportionally scaled down (4:1) with sufficient accuracy from a bridge. In addition, 15 numbers of W sections proportionally in small scale were also being tested. The specimens were 1000 mm long in different levels, sequenced by a loss in the tension flange and induced by notching. The result shows that respectively 51% and 19% increase in flexural strength and stiffness has resulted in composite girders. It also reveals that following after concrete crush the outer CFRP short layer de-bonded prematurely and there was no de-bonding between the inner CFRP layer and steel. The ultimate capacity and stiffness of W sections are reduced by 62% and 45%, respectively due to the complete cutting of tension flanges, whereas insignificant reductions were resulted due to 50% loss of the



flanges. Initially, the recovery of 79% in strength was resulted by CFRP strengthening, but laterally insignificant gains were noticed. The model which is verified for parametric study shows that higher CFRP modulus enhances but enhancement of the flexural strength would be lower due to the reduced inherent tensile strength of CFRPs with the higher modulus.

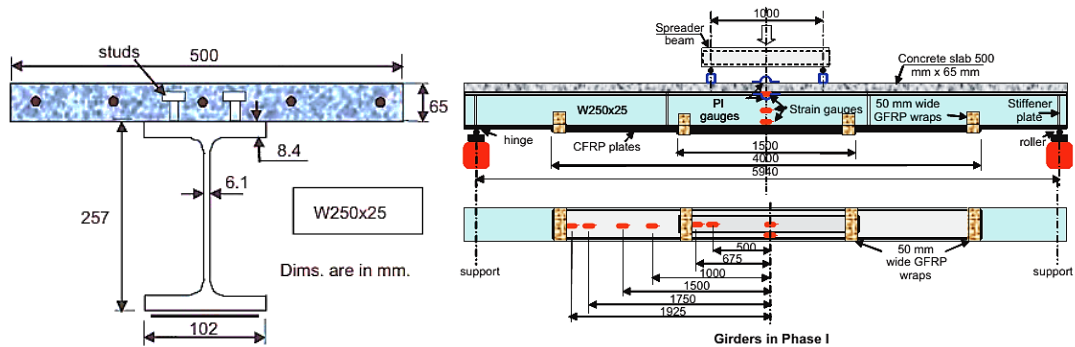


Figure 2.9. Cross section configuration of specimen and test set up [42].

Amr M.I. Sweedan and others [43] in their study proposed an innovative technique by using a special type of drillable fiber reinforced polymer laminates to strengthen the flexural capacity of steel beams. In order to gain both high tensile and high bearing strength hybrid carbon–glass fiber (CFRP–GFRP) pultruded strips laminates are utilized. Their experimental study explores the flexural capacity potential enhancement of steel beams strengthened with mechanically anchored CFRP–GFRP laminates. For the experimental purpose, eleven full-scale beams are considered for flexural testing under three-point loading. The influence of various strengthening parameters is investigated on the behavior including length and thickness of FRP laminates, and a number of anchoring bolts. The experimental result shows that ultimate capacity of the strengthened sections could be improved by increasing length and/or thickness of the FRP laminates. If sufficient numbers of anchors are used, a ductile response associated with high deflection will be exhibited by strengthened beams, otherwise, the shear failure in the anchors which connects FRP laminates to the steel beam will cause a brittle failure.

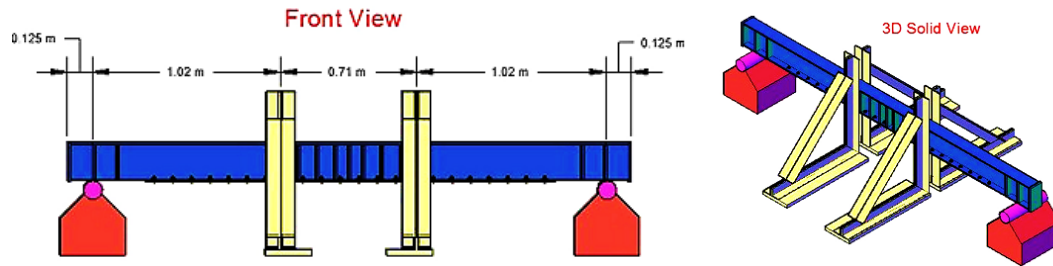


Figure 2.10. Experimental set-up [43].

Hee Sun Kim and Yeong Soo Shin [44] have performed their experimental studies considering the new hybrid Fiber Reinforced Polymer (FRP) system including CFRP and GFRP in order to retrofit the Reinforced Concrete (RC) beams. The main objective of the study concludes the effect of hybrid FRPs observed on the structural behavior of Retrofitted RC beams. In addition, it does investigate whether hybrid FRPs in the form CFRP and GFRP sheets which is placed in different sequences does influence to improve the strength of the RC beam. For the experimental purpose, they have fabricated and retrofitted 14 RC beams with hybrid FRPs considering various combinations of CFRP and GFRP sheets. In order to observe the flexural behavior. Prior to retrofitting, different magnitudes of loading were employed on the Beams in order to notice the effect in the flexure behavior caused by initial loading. Retrofitting of the considered beams is performed by two or three layers of hybrid FRPs depending on loading condition, later on, the load is increased until failure occurs in the beam. The result gained from the study shows that considering hybrid FRPs to strengthen the ductility and stiffness of RC beams is dependent on orders of FRP layers.

## **CHAPTER 3. MATERIAL AND ARRANGEMENT**

The Final Laboratory Experiments, Materials and their applied methods are allocated in the third Chapter. The procedures carried out during the Final Lab experiments are explained step by step with their characteristics and specifications. The preparation scenes of material and specimens are delighted in the form of figures to receive a brief visional pick up of the subject. At the end of this chapter, the set-up of the specimens and the machinery used during all the experiments are introduced briefly with their characteristics and advantages.

### **3.1. Properties Of Materials**

#### **3.1.1. Steel**

The provided steel profile sections used at the final lab test experiments are produced from the A36 type of steel. The specimens considered from the reference steel and heat-treated steel ones are labeled as “Reference” and “Heat Treated” respectively. The material properties of the section are then determined by performing the tensile test for both reference and heat-treated specimens. The size of the test specimens varies depending on different codes and recommendations, but the procedure is almost same for all. [11] Three specimens are considered for the tensile test from each type of steel. The procedure and overall dimensions of the specimen considered for the tensile test is carried out as per ASTM A370-10 standard. The ASTM A370-10 standard dimensions for the specimen are shown in the following figure [45].

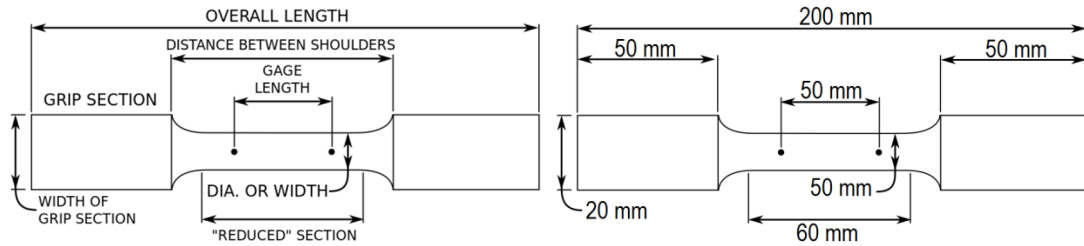


Figure 3.1. Standard dimensions of tensile test specimen.

The most common testing machine used in tensile testing is the universal testing machine, which is introduced in 3.3.2 part of this chapter. The provided specimens are considered under UTM tensile machine for the tensile test (Figure 3.2).

Procedure:

Basically, for tensile test, the specimens of material are placed between two fixtures called “grips” which clamp the material (As shown in Fig. 3.2). The dimensions as length and cross-sectional area of the specimens are selected from recognized standards. Subsequently, the load is applied to specimen kept gripped at one side while the other end is fixed. The load is increased while simultaneously the change in the length is measured for the specimen.

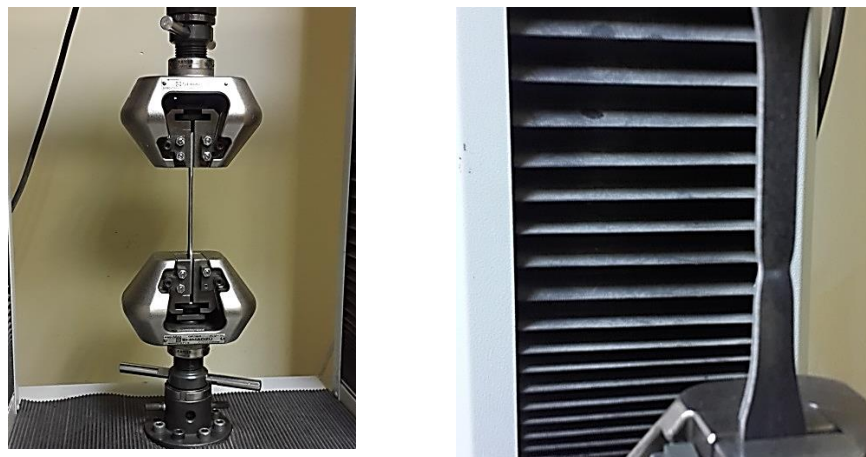


Figure 3.2. Tensile test.

The status of the specimen before and after the tensile test are shown in the form picture at the Fig 3.3 and Fig 3.4.

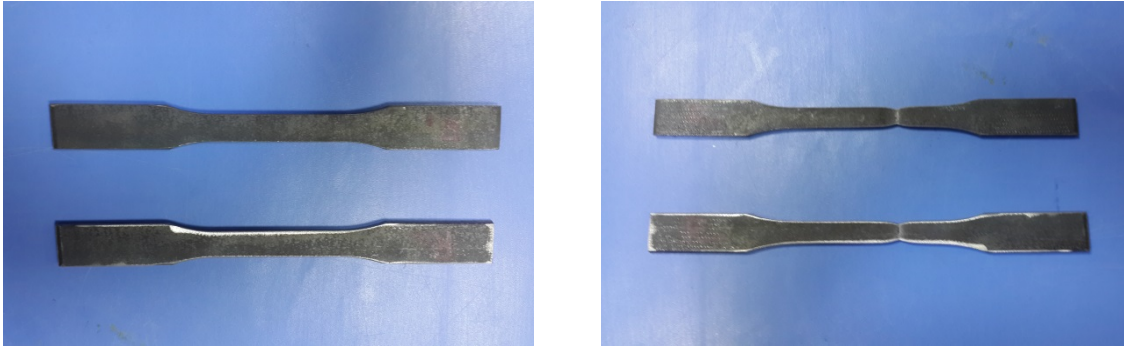


Figure 3.3. Tensile test of reference specimen.

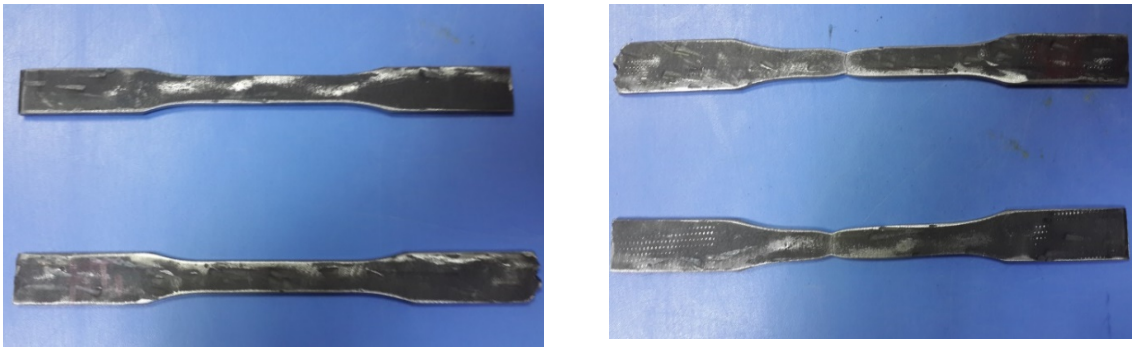


Figure 3.4. Tensile test of heat-treated specimen.

The stress and strain diagram for both Reference and Heat-treated specimens are calculated considering the average values recorded from the group of sets carried out under tensile test. The Stress and Strain diagrams are shown in Fig 3.5.

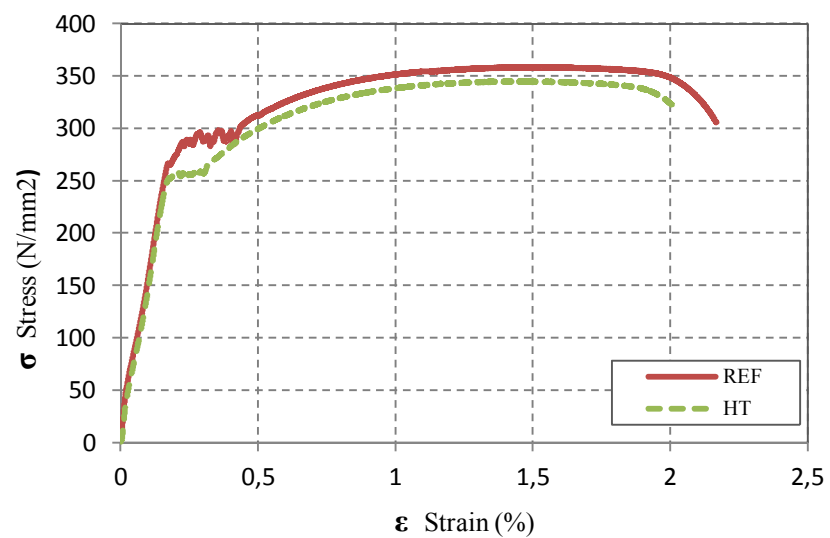


Figure 3.5. Stress and strain diagram for reference and heat-treated specimens.

The test results reveals no change in the elastic modulus property of both reference and heat-treated members. The mechanical properties of specimens are shown in following Table 3.1.

Table 3.1. Mechanical properties of reference and heat-treated specimens

Property	Reference	Heat-treated
Elastic Modules (GPa)	210	210
Yielding stress (MPa)	265	250

### 3.1.2. CFRP

The CFRP plates selected for retrofitting of heat treated specimens are procured from the well-recognized Turkish company called SIKKA YAPI. The company which involves strengthening structural elements and has numerous approvals from many countries in the world for their products claims the following specifications for the mentioned material as [46];

- a. No risk of corrosion
- b. Very high compressive strength
- c. Excellent fatigue strength
- d. Excellent durability
- e. Lightweight
- f. Very easy to install
- g. Requires very little preparation before being applied to the plates

To achieve the mechanical properties of the provided CFRP material, three specimens respectively with the dimensions of 250 mm long, 25 mm wide and 1.2 mm thick have been selected for the tensile test. The dimensions of the specimens are shown in Table 3.2. Dimensions and specifications of the specimens considered for the tensile test meet all the requirements mentioned in the [47-49] references.

Table 3.2. Dimensions of CFRP tensile test specimens

Title	Length (mm)	Width (mm)	Thickness (mm)
CFRP	250	25	1.2

In addition, prior to the test, tabs with the proper length are provided at the both ends of the specimens. Indeed, tabbing a composite specimen is an objective to introduce load into the test specimen without producing premature failure in an undesired failure mode. Thus, production of a valid failure mode within the central gage section of the specimen is due to the successful tab configuration design. [50] The factors and parameters of tabbing a composite specimen are shown in Fig 3.6.

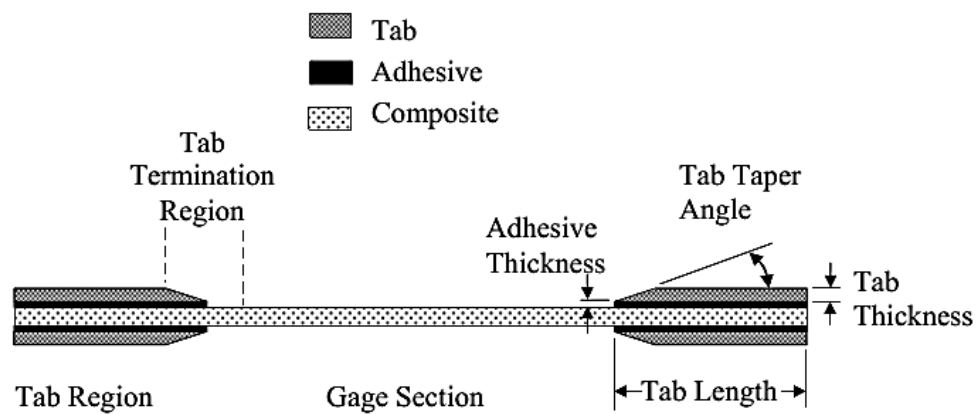


Figure 3.6. Typical tabbed CFRP tensile specimen [50].

Procedure:

The prepared specimens are gripped at the both ends of the apparatus. After wards, the device slowly pulls the specimen longwise on the piece until it fractures.

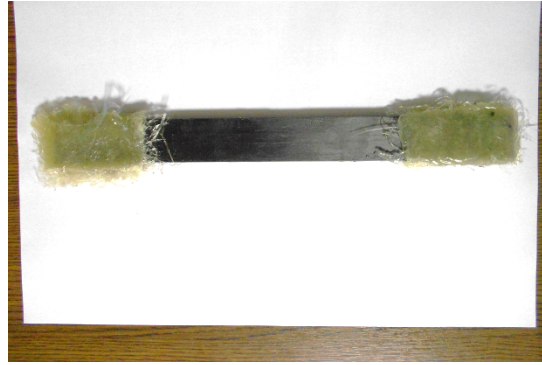


Figure 3.7. CFRP specimen for tensile test.

The behavior of a CFRP specimen after the tensile test is shown in the Fig.3.8.

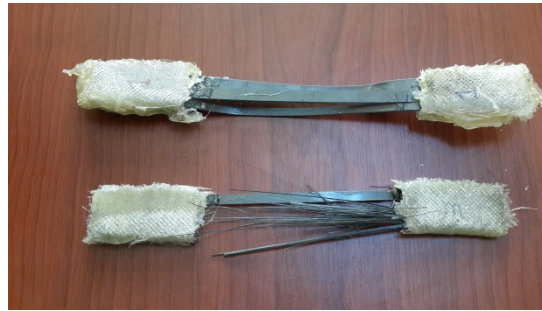


Figure 3.8. Behavior of CFRP specimen after the tensile test.

The pulling force which is called Load is plotted against the material's length change or elongation considering the average of the results received from the group of sets carried out under tensile test. The load and displacements values are later on converted to stress and strain form. The stress and strain diagrams are shown in Fig 3.9.



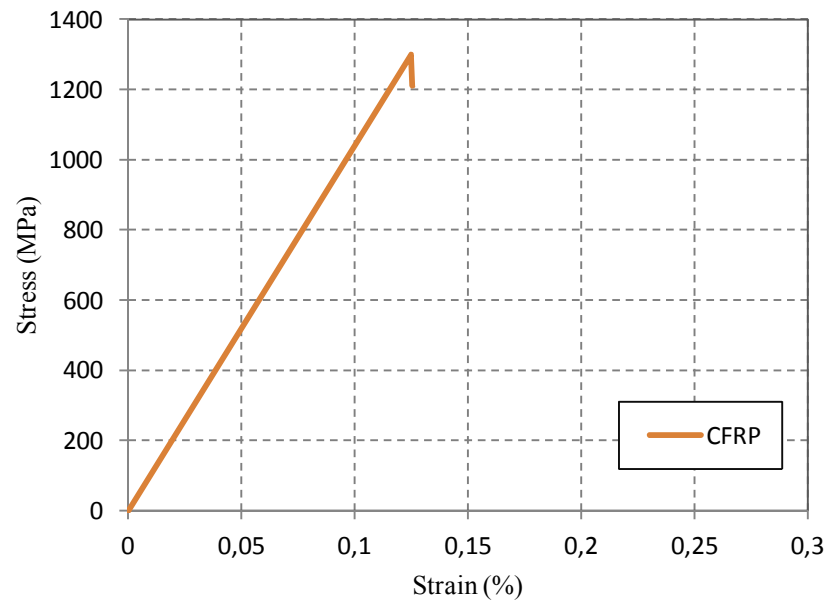


Figure 3.9. Stress and strain diagram for CFRP tensile test specimen.

It is revealed that the carbon fiber composite materials have high tensile strength and modulus of elasticity compared to the other materials. It is also notable that CFRP material shows a brittle behavior and they all break in a brittle manner. According to the diagram, the curve is linear until it fractures without having any bending at the high loads. As a result of the test, no permanent change is seen in the original shape and hence no ductility. The Mechanical properties of the CFRP material received from the tensile test are shown in Table 3.3.

Table 3.3. Mechanical properties CFRP

Title	Reference
Elastic Modules (GPa)	165
Fracture stress (MPa)	1300

### 3.1.3. Adhesive epoxy

Huntsman Araldite AW-106 is selected as adhesive epoxy to join the CFRP plates with the heat-treated beam. Huntsman Araldite AW-106 is suggested to be used for the same instances by Aydin and Aktas [4] in their study. For the purpose to find the

most effective adhesion between CFRP and Steel, Aydin and Aktas has performed a lab experiment on three types of adhesive epoxies, from which are Spabond 345, Köster Chemifix-100 and Huntsman Araldite AW-106. The study reveals that Huntsman Araldite AW-106 has an excellent behavior compared to the others and shows an increase in strength.



Figure 3.10. Admixture of epoxy [4].

The properties related to the Huntsman Araldite AW-106 presented by the producing company are shown in Table 3.4.

Table 3.4. Properties adhesive epoxy

Title	Elastic Modulus (MPa)	Density (gr/cm <sup>3</sup> )
Huntsman Araldite AW-106	1900	1.13

### 3.2. Arrangement of lab works

To observe the behavior of the CFRP for retrofitting the heat treated elements, a sequence of procedures is carried out which is presented respectively in below headings. This part of the chapter will deal with all those arrangements and set ups carried out prior to flexure bending test of a reference and CFRP strengthened beams for the three types of experiments at the laboratory. The specification, properties and working procedure of each step are described with full details including required conditions and norms. In addition, this part also contains a brief introduction to

UTM machine, which is mainly used to apply tensile and flexural bending test on the lab considered specimens.

### 3.2.1. Beam cross section

The IPE 80 which is the smallest available size section among the European standard I sections, is selected for the heat treatment and retrofitting observation. Eight s of IPE 80 beams with the 500 mm length are considered for the test. The specimen which is manufactured from the A36 type of steel is procured from the local company in Turkey. The information provided by the manufacturing company shows that the section is manufactured according to the following Codes and Standards referred below, in addition, the section respectively agrees their conditions [51].

The IPE 80 beam with the parallel flanges is manufactured according to the following standards:

- a. DIN 1025
- b. Euronorm 19-57 (Dimension)
- c. EN 10034: 1993 (Tolerances)
- d. EN 10163-3, C (Surface conditions)
- e. STN 42 5550



Figure 3.11. IPE 80.

In addition, in this study initially, the behavior of the heat treated beam retrofitted by CFRP plates is also considered for detail observation. The section considered in the lab experiment is IPE 80.

Dimensions and properties of IPE 80 are shown in Fig 3.12 and Table 3.6.

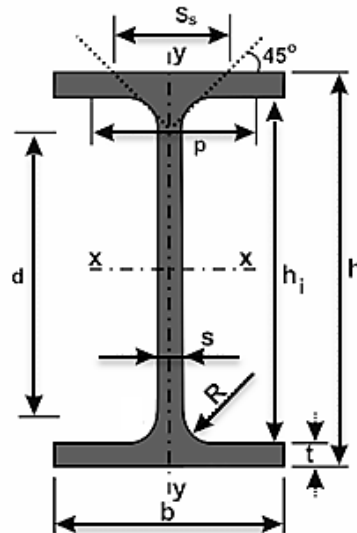


Figure 3.12. IPE 80 steel cross section.

Table 3.5. Dimensions of IPE 80 section

ID	Nominal weight	Nominal Dimensions					Cross-section	Dimensions for detailing					Surface	
		b	h	t <sub>1</sub>	t <sub>2</sub>	R <sub>1</sub>		A	h <sub>1</sub>	d	□	P <sub>min</sub>	P <sub>max</sub>	AL
	Kg/m	mm					cm <sup>2</sup>	mm	mm		mm	mm	m <sup>2</sup> /m	m <sup>2</sup> /m
IPE 80	6	46	80	3.8	5.2	5	7.64	69.6	59.6	-	-	-	0.328	54.64

Table 3.6. Geometrical properties of IPE 80 section

ID	Strong Axis							Weak Axis					
	I <sub>x</sub>	Wel. <sub>x</sub>	Wpl.x	I <sub>x</sub>	A <sub>vy</sub>	S <sub>x</sub>	I <sub>y</sub>	Wel.y	Wpl.y	i <sub>y</sub>	S <sub>s</sub>	I <sub>t</sub>	I <sub>w</sub>
	cm <sup>4</sup>	cm <sup>3</sup>	cm <sup>3</sup>	cm		cm <sup>3</sup>	cm <sup>4</sup>	cm <sup>3</sup>	cm <sup>3</sup>	cm	mm	cm <sup>4</sup>	
IPE 80	80.1	20.0	23.2	3.24	3.58	12	8.49	3.69	5.8	1.05	20.1	0.70	0.12

### 3.2.2. Preparation of steel plates

Prior to the second phase lab experiments (described in 4.3), small size steel plates were considered to observe the CFRP tying behavior with steel plates. Three options are carried out considering a group of hollows with appropriate size and distances only on steel elements and a group of hollows with appropriate size and distances for full bond on both steel plates and CFRP. CFRP fabric strings and tying steel bolts were selected to act as tying elements.

Ten steel plates (Two steel plate from each set of Reference Plate, CFRP retrofitted, CFRP plates along with CFRP fabric strings with half bonding, CFRP plates along with CFRP fabric strings with full bonding and bolt anchorage) respectively 200 mm long, 40 mm wide and 5 mm thick were taken under study. Four holes were drilled on each steel plate and four CFRP plates were drilled for full bond tying observation. The process of the steel plate preparation is shown in the Figure 3.13.

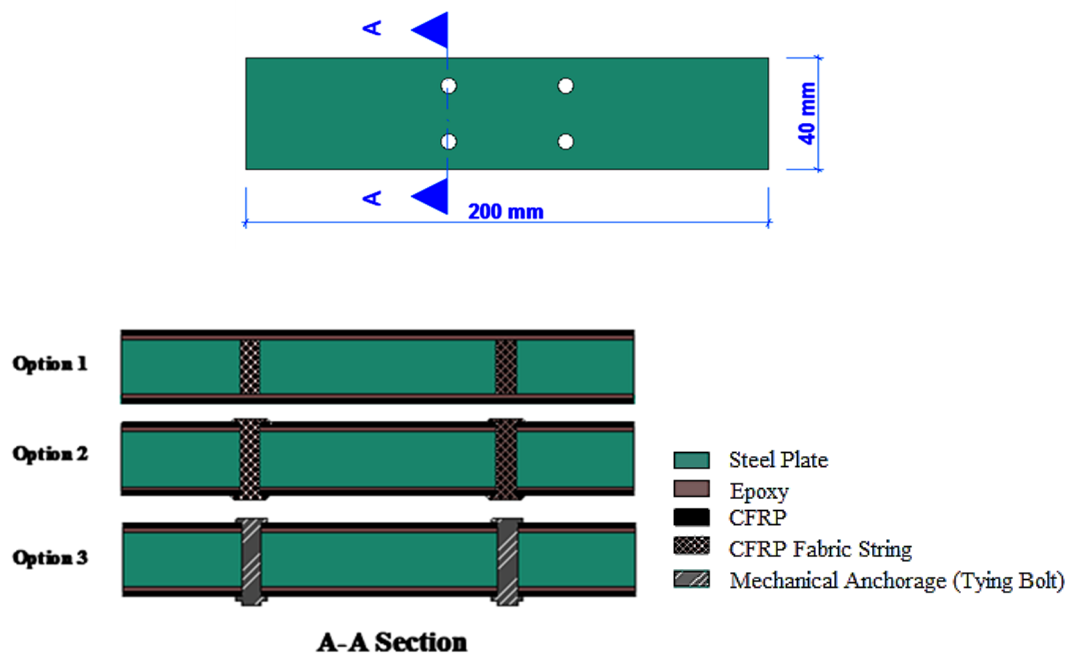


Figure 3.13. Steel plate and tying options.

The drilled steel plates and CFRP plates are later on bonded with epoxy using CFRP fabric and anchorage bolts as shown in Figure 3.14.

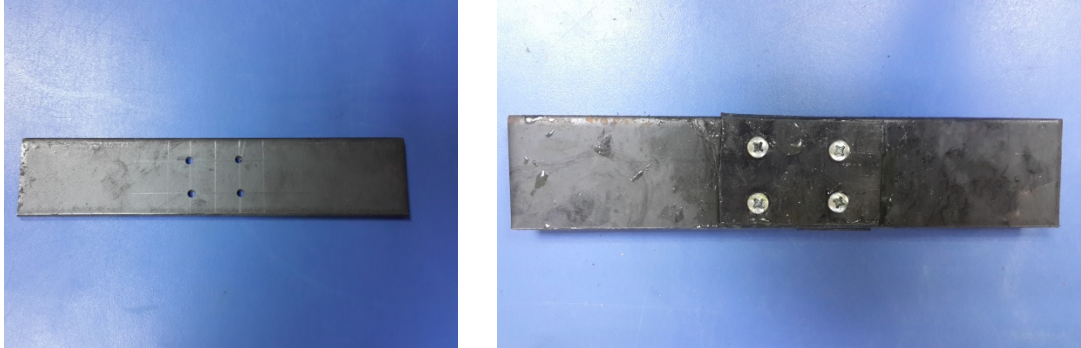


Figure 3.14. Drilled holes in steel plate and CFRP and bolt anchorage.

### 3.2.3. Creating of local deformation

The provided Specimens considered for heat-treatment and CFRP retrofitting are initially locally deformed. The local deformation is occurred through hitting the sides of flanges axially with a hammer. The process is carried out very carefully and it is made sure that no global buckling or global deformation occurs in the section. The length and location of deformation are selected proportionally constant for the entire provided specimens.

The process carried out for creating the local deformations on steel beams and its final shape is shown in Fig. 3.15.



Figure 3.15. Creating of local deformation.

After creating the local deformations on the flanges of the beams, they are controlled whether no cracks rupture or global buckling exists over the section. Finally, after it is being satisfied, the proposed specimens are forwarded to the heat-treatment process.

#### 3.2.4. Mechanical heat treatment

The locally deformed specimens are initially repaired by mechanical heat treatment before applying CFRP plates to the deformed areas. The procedure is carried out to gain the initial geometry of the specimen and increase the strength capacity of the element. The heat repairing is processed by applying Oxy-gas flame to the deformed areas of the specimens. The temperature of heat is kept between 550 to 650 C<sup>o</sup> and to maintain the temperature of heat, the thermocouple device is used to determine the magnitude of the temperature during the heat applied on the deformed element. Later on, the deformed areas are straightened and corrected by pressing the plates of the section.

The entire procedure carried out during the heat treatment of the specimen is shown in the Fig 3.16.



Figure 3.16. Heat treating and straightening of specimens.

The straightened and heat-treated shape of a typical test specimen is shown in Fig 3.17.



Figure 3.17. Straightened and heat-treated shape of test specimens.

### 3.2.5. Drilling holes in flanges

To implement anchorage via bolt tying, the heat-treated beams are considered for drilling holes. Six holes with 4 mm diameter in two rows and 3 columns perpendicular to each other are drilled for each provided heat-treated beam.

The heat treated steel beam positioned for drilling producer is shown in the Fig 3.18.



Figure 3.18. Drilling procedure for steel beam.

### 3.2.6. Installation of CFRP

CFRP plates with different dimensions were trimmed to observe the efficiency of the different locations arrangements and type of CFRP anchorage employing on the flexure strength behavior of heat-treated beam. Later on, the admixture of suggested



epoxy with an appropriate ratio was prepared at the room temperature. The tying surfaces were prepared and cleaned before bonding the steel and CFRP with epoxy; thus it was made sure that no moisture and corrosion exists on the bond surfaces; In addition, the surfaces of steel bonding areas were ground for a better result. The prepared epoxy admixture was applied to the CFRP surfaces with a constant thickness.

Implementing bolt anchorage and the process of applying epoxy to the face of the specimens are shown in the Figure 3.19.

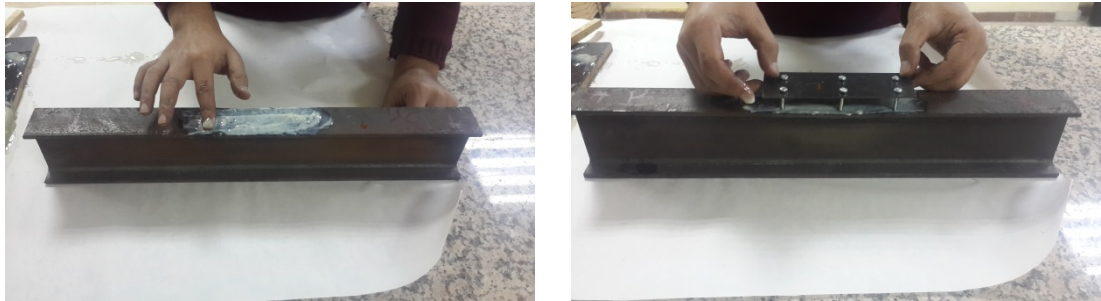


Figure 3.19. Applying epoxy & CFRP on the face of specimens.

Finally, the epoxy applied CFRP plates were bonded to the ground surfaces of steel specimen and to scatter the epoxy homogeneously along the entire bonding area, the bolts were screwed and the specimens were kept tied by clamp tools. See Fig 3.20.



Figure 3.20. Employing bolts & clamping the specimens.

To get more hard and tight bonding between the elements, the specimens cured and kept tight with the clamps as per the guidance prescribed at norms and epoxy

providing company. The specimens shown in the Fig 3.21 are ready to be considered for a lab test.



Figure 3.21. The specimens ready for lab experiment.

### 3.3. Test setup

The machinery and devices used in the lab experiment are briefly introduced here.

#### 3.3.1. Universal testing machine (High capacity)

The Universal Testing Machine UTM which is also called as a materials testing machine is considered to examine the tensile and compressive properties of materials. The application of the machine is to investigate Compression, tension, bending etc. and mechanical properties of materials. Generally, it is supported on two columns but single column types could also be found. The computer operating type of UTM machine can present the graphical mode of force and deformation which is the main key parameters of these tests. Recently UTM machines are widely used around the world and most of the material testing laboratories possess this machine [52].

The available UTM machine at the Sakarya University Engineering Lab is the product of a Turkish company called the AŞLAN Company and has the following properties.

Description of the product: Computer-controlled, Hydraulic loading, Materials testing software and Comply with EN ISO 10002-1 TS 138.

Capacity: 40 TONS / 400 KN

Type of tests: Tension, Compression, Bending and Load Hibernating



Figure 3.22. AŞLAN UTM machine [52].

### 3.3.2. Universal testing machine (Low capacity)

This device is used during the preliminary test carried out to (See 4.2. Part) choose the most effective type of anchorage for the retrofitting purpose. Indeed, this device is used for low capacity bearing elements test [53].

Description of the product: AG-IC Table-Top Type, Computer-controlled

Capacity: 20 / 50 KN

Type of tests: Tension, Compression, Bending and Load Hibernating



Figure 3.23. AG-IC Table-Top type UTM [53].

### 3.3.3. Drilling machine

Description of the Product: Optimum B 20

Capacity: Max drilling  $\varnothing$  20 mm



Figure 3.24. Optimum B20 drilling machine [54].

## **CHAPTER 4. LAB STUDIES**

The Fourth Chapter describes the deforming behavior of the I Beam under the concentrated load carried out during the experiment. The behavior and load capacity of the deformed steel I Beams are observed after the heat treatment compared to its initial load bearing state. Later on, the specimen is strengthened with CFRP for retrofitting and permanent repairing, the behavior and impact of CFRP is studied from the results of the experiments. All these states are figured and compared in the form of force and displacement graphs.

The Lab experiments are carried out in three different stages. The first stage which deals with heat treated IPE 80 beam is considered for retrofitting purpose. The result received from this stage (Refer to section 4.1) induces us to carry the same experiment considering a restraining element to CFRP and Steel plates to resist more force. Initially, steel plates bonded by epoxy with CFRP plates and restrained with CFRP fabric and tying bolts are considered under lab experiment. Subsequently after observing the result revealed from the steel plates, the most effective type of tying element is selected for the conclusive experiments (Refer to section 4.2). Finally, the scaled IPE 80 beam is taken under study while restrained with tying bolts.

During the experiments the specimens' names were abbreviated with some characters that respectively stands for, "RB" Reference Beam, "HT" Heat Treated, "C" CFRP retrofitted, "C1, C2, C3" location arrangement of CFRP, "SPcr" Steel plate only CFRP retrofitted, "SPre" Steel plate reference, "SPbr" Steel plate bolt restrained, "SPcrh" Steel plate CFRP fabric half restrained, "SPcrf" Steel plate CFRP fabric full restrained, "RBbr" Reference beam bolt restrained.

## **4.1. Initial Experiment**

As initial experiment IPE 80 is subjected to three-point bending test. The procedure carried out during lab experiment is the same with the Final Experiment. However different CFRP arrangements as shown in Table 4.2 have been considered. Totally 10 s of IPE 80 steel profile section (Sets of the Reference beam, Heat treated and CFRP retrofitted) having 500 mm length are considered for lab experiments while carrying a different arrangement of CFRP location.

### **4.1.1. Reference and heat-treated IPE 80 beams**

Two specimens of IPE 80 steel beam having 500 mm length are taken under study to derive comparison of load capacity between the original reference beam and heat-treated one. The heat-treated one is initially locally deformed and subsequently, after heat-treating three points bending load test is applied to find the capacity of the beam after the heat-treatment process.

Procedure:

The provided specimens are placed on two supporting pins with a set of 400 mm distance apart, later on from the above direction, the third loading pin is lowered with a constant rate until the specimen failure. During the test, the applied load and displacements are recorded and shown in the form of a graph.

Finally, for the comparison purpose, the graphs are brought together as shown in Fig 4.1.

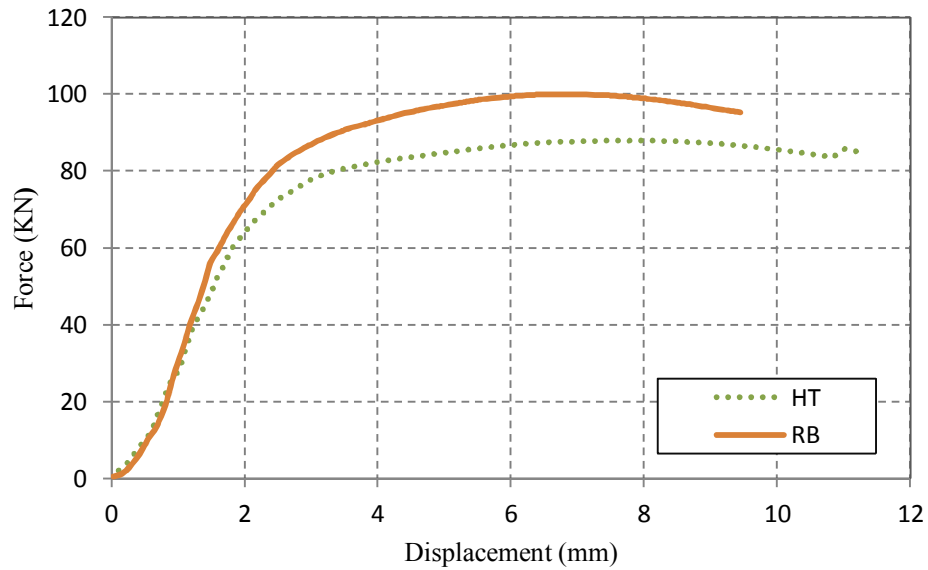


Figure 4.1. Force-displacement graph for IPE 80 RB and HT specimens.

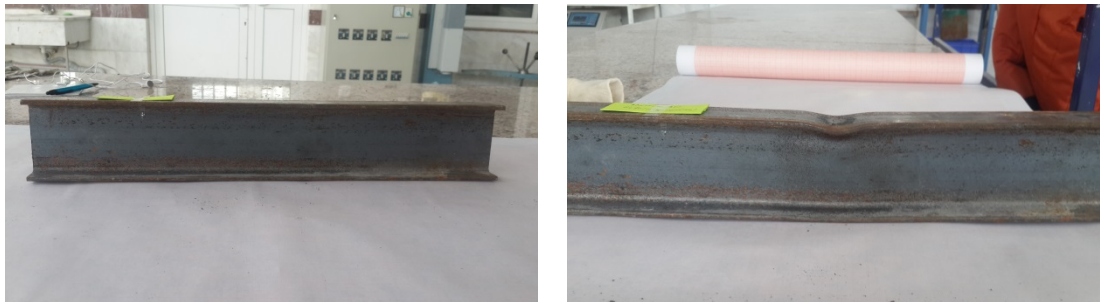


Figure 4.2. IPE 80 Reference beam before and after the test.

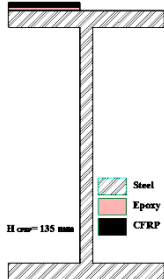


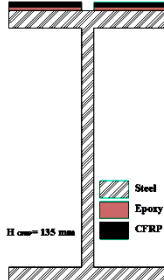

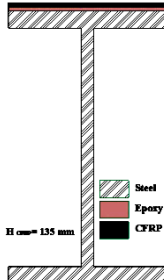


The results reveals that heat-treatment causes the loss of section load capacity compared to the reference section. The load capacity of a heat-treated section respectively decreases about 20% compared to the reference beam which requires to be retrofitted by re-strengthening elements as CFRP.

#### 4.1.2. CFRP retrofitted IPE 80 beams

Eight IPE 80 steel beam specimens having 500 mm length are taken under study to derive the comparison of load capacity compare the original reference beam. The provided CFRP retrofitted IPE 80 beams having different CFRP allocation arrangement (See Table 4.1) are taken under three points load test.

Mainly three types of CFRP arrangement are considered while bonding with the section of steel flanges in this step of the experiment, which is one sided, double sided (two parts) and double sided (one part) CFRP plates. The arrangements are shown in Table 4.1.

Table 4.1. Arrangement of CFRP plates

ID	Section	Prior to test	After the test
HTC1			
HTC2			
HTC3			

#### Procedure:

The considered specimens are located on two supporting pins with a set of 400 mm distance apart; the loading is applied from the above direction by lowering the third loading pin with a constant rate until the specimen failure. The applied load and displacements are recorded during the test and shown in the form of a graph. The same procedure is carried out for all these above-mentioned beams.



Finally, for the comparison purpose, the graphs are brought together as shown in Fig 4.3. The graphs for the HTC1, HTC2, and HTC3 are respectively figured from the Specimen 9, Specimen 5 and Specimen 6.

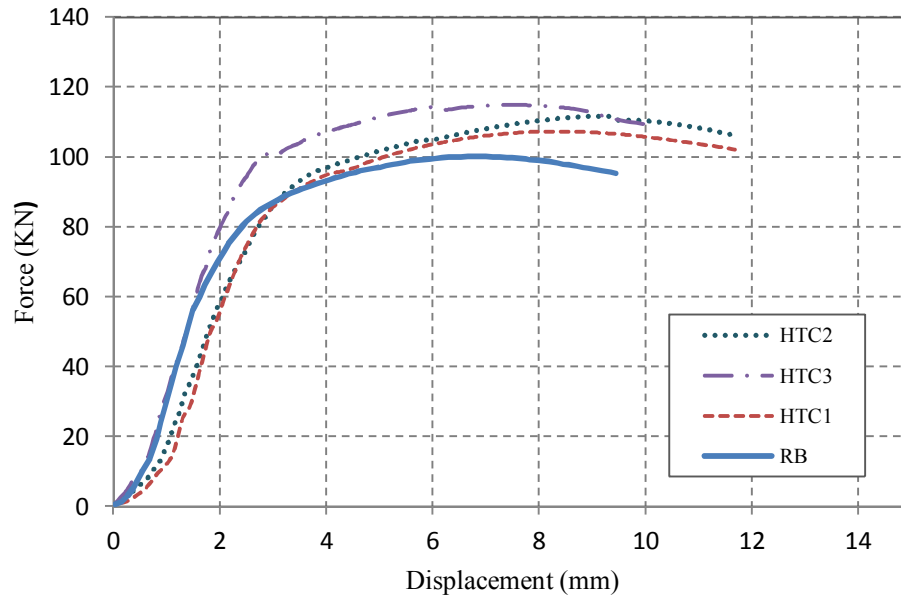


Figure 4.3. Force-displacement graph for IPE 80 RB & carbon retrofitted

As a result, it is being revealed that the load capacity and displacement of the CFRP retrofitted element has been respectively increased with an average of 8.35% and 8% compared to the original Reference beam.

In addition, it is also being observed during the experiments that epoxy scatters formerly than CFRP while resisting load and hence it causes to prevent the specimen to sustain much more load. Hence as a conclusion it is decided if the CFRP plates are anchored to the epoxy bonded steel flanges, it will cause the CFRP to resist more force and develop the load capacity of the beam compared to the only epoxy bonded CFRP retrofitted steel beam, so therefore this concept endorses us to carry out the similar experiments procedure with additional anchorage used to connect the CFRP plates with the steel elements.

## 4.2. Choosing Type Of Anchorage

Prior to anchoring the CFRP plate to the steel element in the final stage of experimental study, it is necessary to select the type of anchor. Generally, three concepts as shown in the Fig. 4.4 are taken into consideration, which are as below;

Option 1: CFRP fabric string half tied (bonded from interior faces of CFRP)

Option 3: CFRP fabric string full tied (bonded from exterior faces of CFRP)

Option 3: Tying bolts

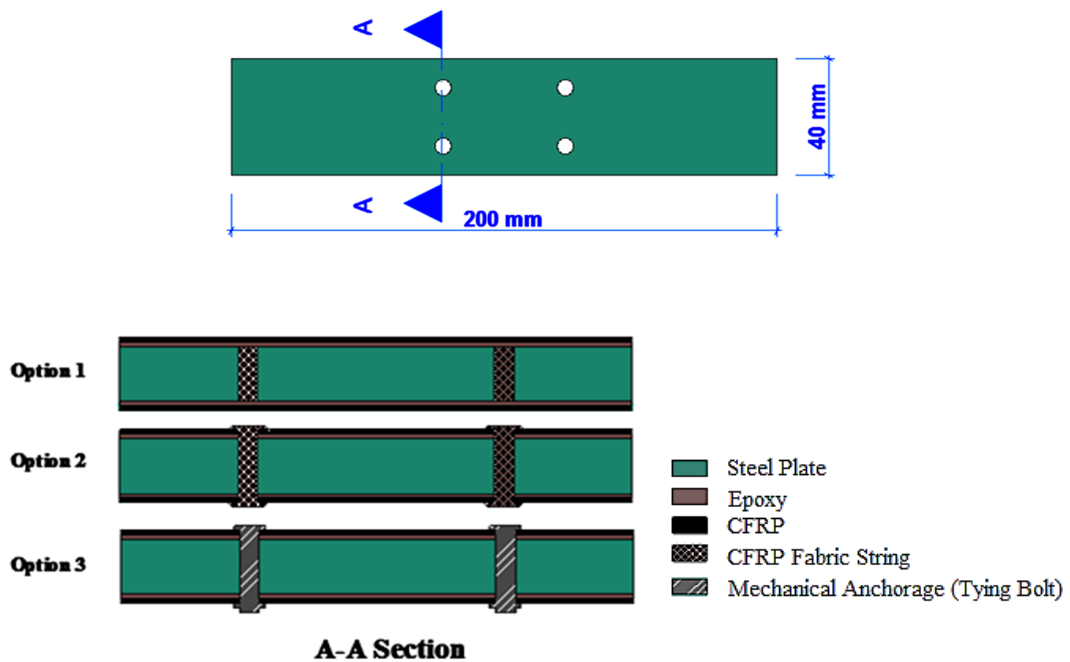







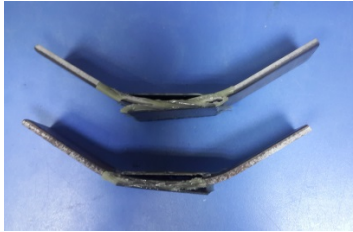





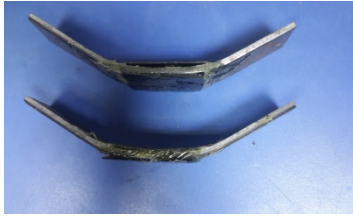



Figure 4.4. Types of anchorage.

Properties of materials and experiment arrangement are provided respectively in Chapter 2 and Chapter 3. Totally 10 steel plates (as shown in Table 4.2) having 200 mm length are considered in the experimental study while having a different arrangement of anchor tying as described above.

Procedure:

The provided specimens (as shown in Table 4.2) are placed on two supporting pins with a set of 150 mm distance apart, later on from the above direction, the two loading pin is lowered with a constant rate until the specimen failure (as shown in Fig 4.5 ). The same procedure is carried out for all these provided plates.

Table 4.2. Arrangement of steel shell plates

ID	Section	Prior to test	After the test
SPre			
SPcr			
SPcrh			
SPcrf			
SPbr			

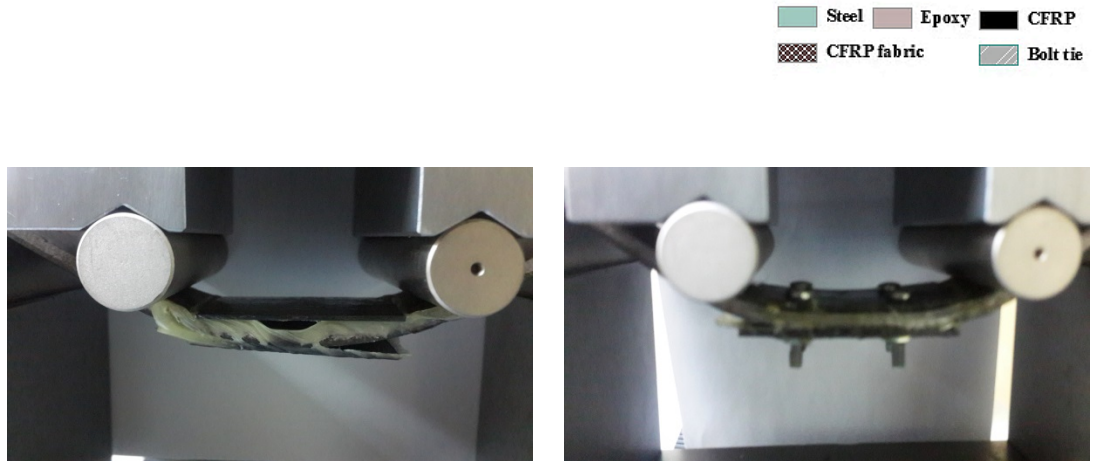


Figure 4.5. CFRP retrofitted steel plates under four-point bending test.

During the test, the applied load and displacements are recorded and shown in the form of a graph. The graphs for each type of specimens are plotted from the average of their respective results. Finally, for the comparison purpose, the graphs are brought together as shown in Fig 4.6.

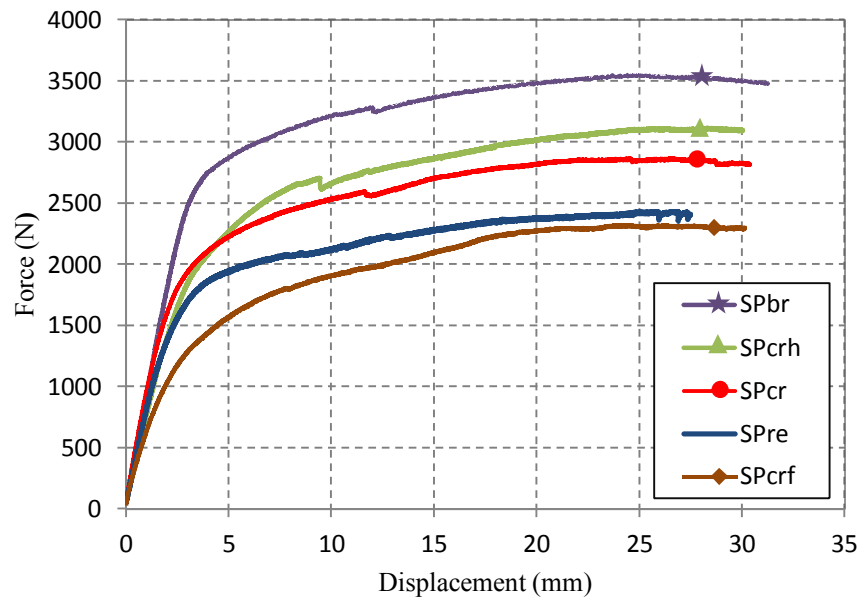


Figure 4.6. Force-displacement graph for steel plates specimens.

Tests on the steel plates with different (additional)anchorage details, reveals that employing bolt anchorage provides better bonding behavior compared to the others

(See Figure 4.6 above) and causes the CFRP plates to resist larger load. Subsequently, bolt anchorage is considered to be employed as tying element of CFRP plates in the next stage experiment study on IPE 80 specimens.

### **4.3. Final Experiment**

IPE 80 profile section is observed under three-point bending test in this part of lab experiments. Properties of materials and experiment arrangements are provided respectively in Chapter 2 and Chapter 3. Totally 10 steel beam with IPE 80 cross sections having 500 mm length are considered for lab experiments, all of which own a different arrangement of CFRP bonding to steel flanges.

The provided CFRP retrofitted IPE 80 beams having different CFRP bonding arrangements (See Table 4.1) are taken under three-point bending test.

#### **4.3.1. Reference IPE 80 beam**

Two IPE 80 specimens steel beams as a set having 500 mm length with the same properties are taken under study to derive the load capacity of the original reference beam that is not subjected to any heat treatment. The considered specimens are initially located on the supporting pins of UTM device for the application of three-point bending test.

The applied load and displacement of the specimens during the test is recorded and finally, the load capacity parameters of the specimen are represented in the form of Force and Displacement graph as shown in the Fig. 4.8.

The shape of reference beam before and after the experimental test is shown in the Fig. 4.7 below.



Figure 4.7. Reference beam before and after the test.

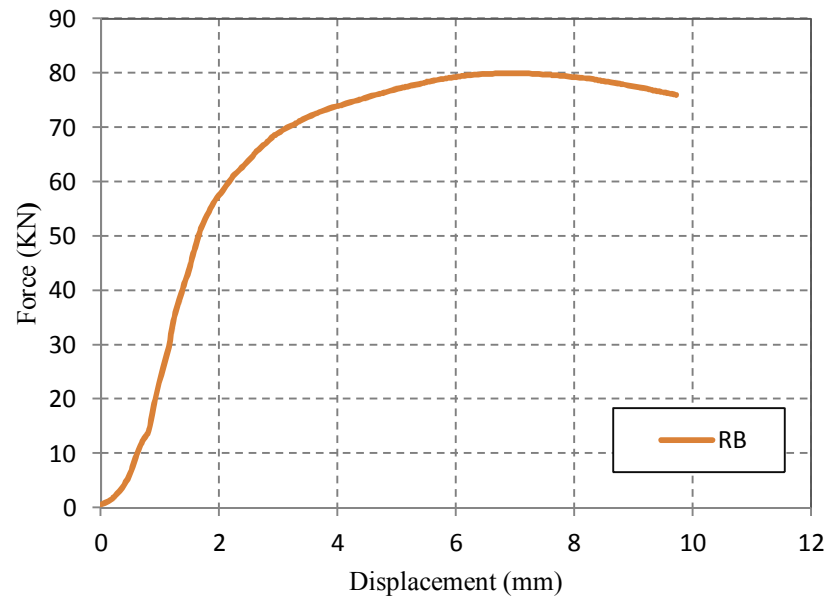


Figure 4.8. Force-displacement graph for reference beam.

#### 4.3.2. CFRP and mechanically retrofitted IPE 80 beams

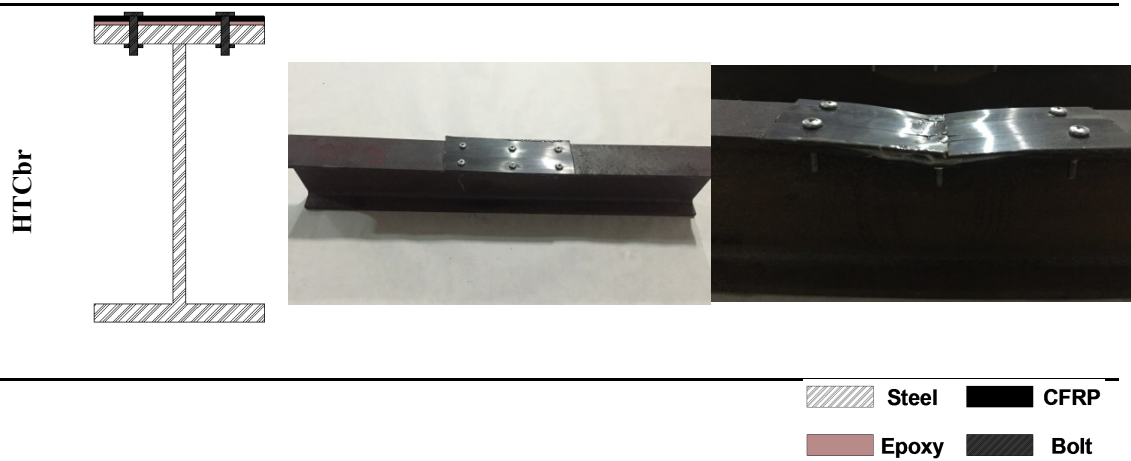
Eight IPE 80 steel beams specimens having 500 mm length are taken under study to derive the comparison of load capacity of the retrofitted specimen compare to the original reference beam. The provided CFRP retrofitted IPE 80 beams having different CFRP bonding arrangements (See Table 4.1) are taken under three-point bending test (See Fig. 4.9). Mainly two types of CFRP arrangement to be bonded with the flanges of the steel section are considered in this part of the experiment, both of which are CFRP with the only epoxy bonded and CFRP with bolt anchorage epoxy bonded.



Figure 4.9. Retrofitted beams under three-point bending test.

Table 4.3. Arrangement of CFRP plates

		Experimental materials			
		Reference Steel	Heat-Treated Steel	CFRP	Adhesive
Modulus of Elasticity (MPa)		210,000	210,000	165000	19,000
Yield Strength (MPa)		265	250	-	-
Density (g/cm <sup>3</sup> )		7.85	7.85	1.62	1.13
ID	Section	Prior to test		After the test	
RB					
HTCr					



Procedure:

The provided specimens are placed on two supporting pins with a set of 400 mm distance apart, later on from the above direction, two loading pins are lowered with a constant rate until the specimen failure. During the test, the applied load and displacements are recorded and shown in the form of a graph. The procedure is carried out the same for all these provided specimens. Finally, for the comparison purpose, the graphs are brought together as shown in Fig4.10 and Table 4.4. The graphs for the RB, HTCcr, and HTCbr are respectively figured from the average of the given sets.

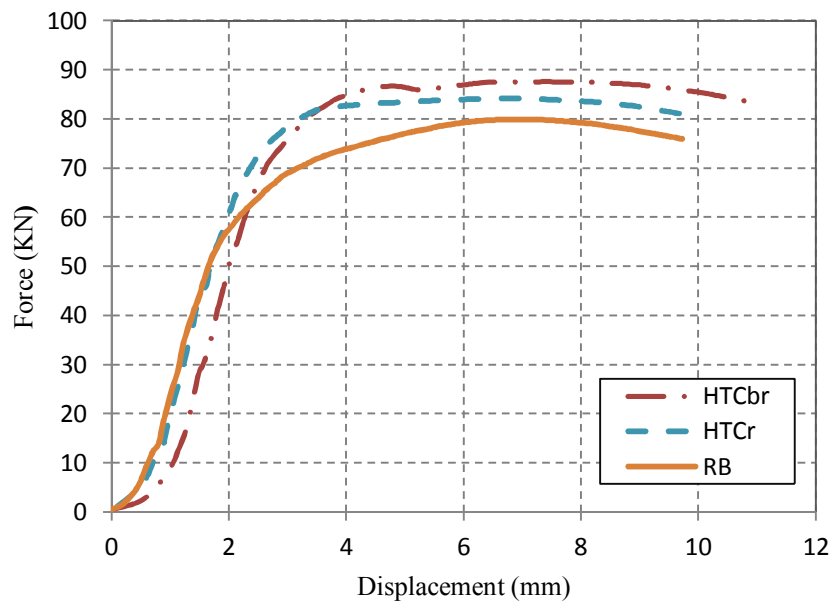




Figure 4.10. Force-displacement graph of reference and retrofitted beams.  
 Table 4.4. Lab experimental results

ID	Lab Experimental Results		
	Max Load (KN)	Max. displacement (mm)	Load Difference %
RB	80	9.7	-
HTCr	84	11	5
HTCbr	88	11.5	10

As a result, it has been observed that employing bolt anchorage along with epoxy bonding to the heat-treated areas of a deformed specimen causes the element to resist much more load and shows a good behavior compared to its other counterparts.

## **CHAPTER 5. VERIFICATION OF FEM MODAL**

The Chapter 5 will explain the manner and characteristics of the Finite Element Program ABAQUS for modeling the steel beams. The specification and modeling of materials used in the experiments are provided with their detailing.

The Finite Element Method (FEM) is approximately a proper method while considering a parametric study on bigger size specimens. Hence this method impacts economically effective on the budget of the lab experiments and most importantly saves much more time. This method could only be applicable for parametric study after verifying the performed lab test with the FEM modal analysis.

Besides, it is important to define the geometric imperfection of the specimen for the nonlinear analysis in the FEM modeling. Prior to the nonlinear analysis of the specimen, the shell elements should be considered for geometric imperfection option by defining buckling modes to the analysis [55].

The FEM analyses are carried out in ABAQUS software which is mostly used for analyzing the linear and nonlinear problems. A perfect and potential solution for both type of engineering problems (routine or sophisticated). is offered by the ABAQUS Unified FEA product suite. It covers massive spectrum applications of the industries, for instances, the engineering workgroups of an automotive industry can consider full vehicle loads, multibody systems, dynamic vibration, nonlinear static, impact/crash, acoustic-structural coupling, and thermal coupling by using a common model data structure and integrated solver technology. To gather the processes and equipment, decrease costs and inefficiencies, and enhance a competitive advantage, well-recognized companies prefer to use ABAQUS Unified FEA [56].

In the conclusion part of this Chapter, the output result received from the ABABUS program is initially reviewed and later on, they are compared with the results received from the lab experiments for the verification.

## **5.1. Modeling Of Materials**

The mechanical properties of the entire materials presented in the lab experiments are defined with considering the real behavior of the material in FEM modeling.

Totally three types of materials are defined in this FEM modeling, which is Steel, Epoxy, and CFRP. The mechanical and numerical specification of each material is described respectively with details.

### **5.1.1. Steel**

The behavior of structural steel under static and tensile forces could be specified by modifying the mechanical properties of the material, such as Elastic modulus, tensile stress and passion ratio in FEM models. These parameters could be received by performing the tensile test for the considered material.

The stress and strain curve of the structural steel is shown in Figure 5.1.

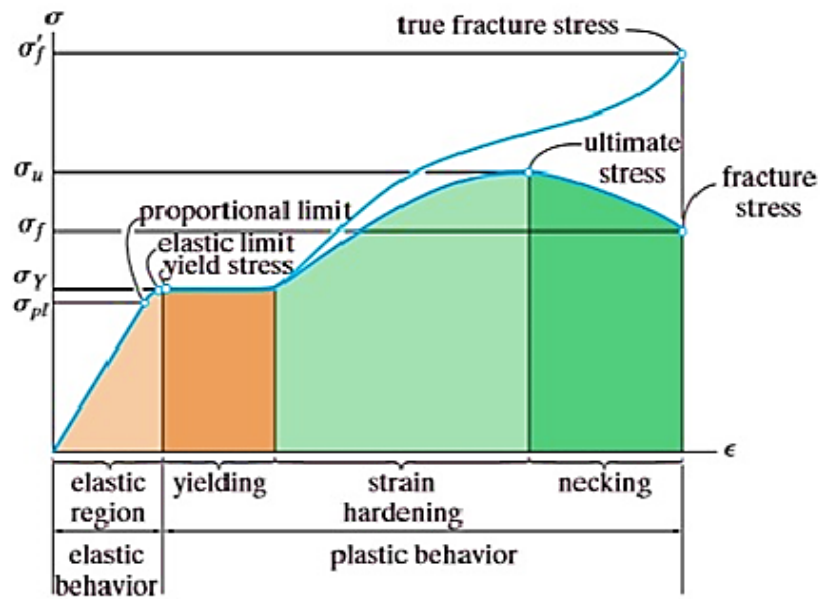


Figure 5.1. Conventional and true stress and strain diagrams of steel [57].

The property of Steel material is defined as ideal elastic-plastic behavior in this modeling. The Elastic-Plastic Stress and Strain diagram is formed from two parts as shown in Figure 5.2.

$$\sigma = E \cdot \varepsilon \quad \text{for} \quad 0 < \varepsilon < \varepsilon_e$$

$$\sigma = \sigma_y \quad \text{for} \quad \varepsilon_e < \varepsilon < \infty$$

The contents of the above equation respectively stand as for,  $\varepsilon_e$  the Elastic unit displacement,  $E$  the elastic modulus of the material and  $\sigma_y$  is the yielding stress of the material. In addition, the compression and tensile behavior of the material are considered the same in modeling.

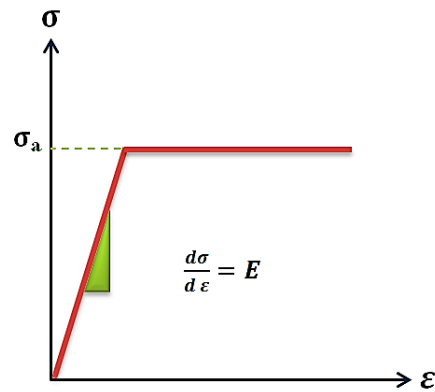


Figure 5.2. Ideal elastic-plastic behavior of materials.

The literature [55] concerning FEM analysis suggests a decrease about 27.56 MPa to be considered between the dynamic and static analysis test results. The property of the reference and heat treated steel are described and shown in chapter 3 Figure 3.5.

The mechanical property of the material considered for FEM model analysis is shown in Table 5.1.

Table 5.1. Mechanical property of steel for FEM models

Element type	E (GPa)	$\mu$ (Poisson ratio)	$\sigma_a$	Density ( $t/mm^3$ )
Steel	210	0.3	265	1.13-10

### 5.1.2. Adhesive material

The adhesive materials are used to bond the steel with the FRP materials to work together and avoid their separation during load appliance. For the purpose, the cohesive materials provided in FEM are selected to maintain collaborative response and to transfer the stresses beyond the elements.

Linear Elastic Traction-Separation Behavior:

The traction- separation model provided in ABAQUS, initially considers linear elastic behavior followed by the initiation and evolution of damage. The elastic behavior is modified in the form of a constitutive matrix. This matrix relates the matrix and shear stress to the normal and shear stresses of the cracked elements. The vector of nominal traction stress consists of  $\mathbf{t}_n$ ,  $\mathbf{t}_s$  and (in three-dimensional problems)  $\mathbf{t}_t$ , which respectively represent the normal and the two shear tractions.  $\mathbf{K}_{nn}$ ,  $\mathbf{K}_{ss}$  and  $\mathbf{K}_{tt}$  terms for an enriched element could be calculated based on the elastic properties. The corresponding separations are denoted by  $\boldsymbol{\varepsilon}_n$ ,  $\boldsymbol{\varepsilon}_t$  and  $\boldsymbol{\varepsilon}_t$ . The equation (5.1) illustrates the elastic behavior as [56].

$$\mathbf{t} = \begin{Bmatrix} t_n \\ t_s \\ t_t \end{Bmatrix} = \begin{bmatrix} \mathbf{K}_{nn} & \mathbf{0} & \mathbf{0} \\ \mathbf{0} & \mathbf{K}_{ss} & \mathbf{0} \\ \mathbf{0} & \mathbf{0} & \mathbf{K}_{tt} \end{bmatrix} \begin{Bmatrix} \boldsymbol{\varepsilon}_n \\ \boldsymbol{\varepsilon}_s \\ \boldsymbol{\varepsilon}_t \end{Bmatrix} = \mathbf{K}\boldsymbol{\varepsilon} \quad (5.1)$$

Normal stresses for each point of integration could be found through dividing the force components by the original area. The nominal displacement for each point of integration could be derived through dividing the traction length via the original thickness. The initial thickness of the element is considered as  $t_c=1$ , unlike the module of the elasticity should be divided by the thickness of the elements [56].

The thickness of the element in this model is selected as 0.1 units. The provided value is derived from the principles described above. The suggested type of cohesive element modeling by FEM is shown in Figure 5.3.

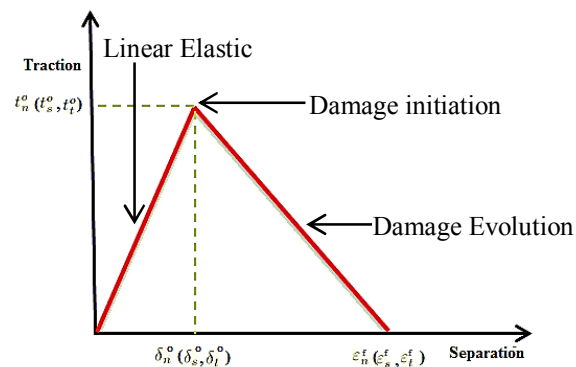


Figure 5.3. FEM suggested model.

The properties of the cohesive material for FEM purpose is shown in Table 5.2

Table 5.2. Properties of cohesive elements

Element type	E (GPa)	G1(MPa)	G2(MPa)	Denisty (t/mm <sup>3</sup> )
Epoxy	19000	6333	6333	1.13 E-10

As discussed earlier that the initial response of the cohesive element is assumed to be linear. However, material damage can occur according to a user-defined damage evolution law once damage initiation criterion is met. The damage initiation is defined as Quadratic nominal stress criterion. Damage is assumed to initiate when a quadratic interaction function involving the nominal stress ratios reaches a value of one. This criterion can be represented as [56]:

$$\left\{ \frac{t_n}{t_n^0} \right\}^2 + \left\{ \frac{t_s}{t_s^0} \right\}^2 + \left\{ \frac{t_t}{t_t^0} \right\}^2 \quad (5.2)$$

In the above discussion,  $t_n^0$ ,  $t_s^0$  and  $t_t^0$  demonstrate the peak values of the nominal stress at the time the deformation is either purely normal to the interface or is purely in the shear direction; respectively first or the second [56] .

### 5.1.3. CFRP

The CFRP plates detach from the steel surface while epoxy starts to scatter. Due to this separation, no defect occurs to the CFRP plates and this behavior is also considered for CFRP in FEM model. For the purpose, the CFRP is modified as elastic linear material to FEM. The properties of CFRP are shown in (Table 5.3).

Table 5.3. Properties of CFRP elements

Element Type	E (MPa)	Denisty (t/mm <sup>3</sup> )
CFRP	165000	1.62 E-9

## 5.2. Types Of FEM Elements

The fundamental components in the ABAQUS model are finite elements and rigid bodies. Finite elements are deformable, whereas rigid bodies move through space without changing its shape. ABAQUS contains a wide range of finite elements and the degree of the freedom (dof) of the element is the fundamental variable during the analysis.

Displacements, rotations, temperatures, and the other degrees of freedom are calculated only at the nodes by obtaining linear interpolation in each direction or using quadratic interpolation of the element. The expressions as Full and reduced integration are available in ABAQUS to integrate the polynomial terms in an element's stiffness matrix. Fully integrated polynomial term respectively use two and three integration points in each direction for linear and quadratic elements as shown in (Figure 5.4).



Figure 5.4. Fully integrated linear and quadratic elements [56].

Unlike fully integrated elements, the reduced-integration elements use one fewer integration point in each direction. There is only a single integration point located at the element's centroid for linear elements of reduced-integration. To observe the displacements and its accuracy in plasticity, this type of integration is used in the analysis. The locations of the integration points for linear and quadrilateral elements of reduced-integration are shown in (Figure 5.5.).





Figure 5.5. Reduced integrated linear and quadratic elements [56].

There is a wide range of elements available in FEM, hence in this study, two types of elements are chosen from the ABAQUS library, both of which are 2-dimensional shell element (S4R) for steel and CFRP, 3-dimensional cohesive element (COH3D8) for epoxy [56].

### 5.2.1. S4R element type

S4R is a 4-node, quadrilateral, stress/displacement shell element that has reduced integration and a large-strain formulation (Figure 5.6). S4R can be used for problems prone to membrane or bending mode hour-glassing, in areas if greater solution accuracy is intended or in-plane bending is expected for the problems anywhere. [56]

The steel profile and CFRP plates are modeled by using an S4R type of element. Modeling this type of elements provided an accurate output result.

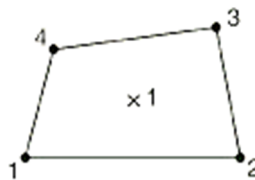


Figure 5.6. S4R element type [56].

### 5.2.1. COH3D8 element type

The convention in order to name cohesive elements used in ABAQUS is demonstrated in Figure 5.7.

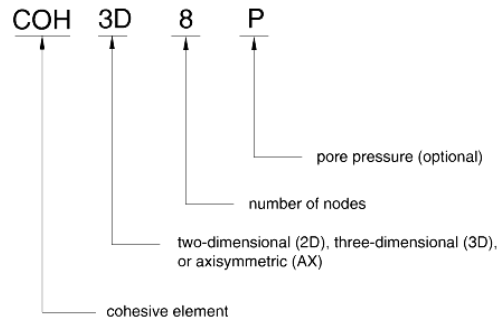


Figure 5.7. Naming convention of cohesive elements [56].

The COH3D8 has 8 nodes with 4 nodes of integration as shown in (Figure 5.8). The active degrees of freedom for the adhesive material is the normal translational freedom component and sliding freedom components in both directions.

The adhesive material used as bonding material is modeled by using a COH3D8 type of element in this study.

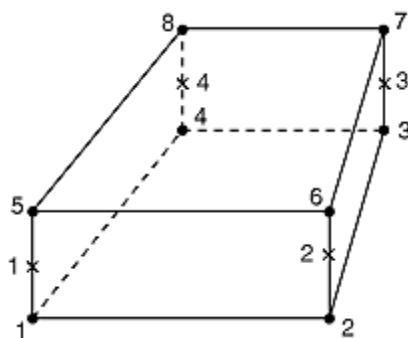


Figure 5.8. COH3D8 element type [56].

### 5.3. Boundary Conditions

The subject beam in the model has two types of support constraints. The degree of the freedom to fix support of model beam is constrained with 3 nodes of rotation and 2 nodes of translational, while the degree of freedom to the roller support of the model is constrained with the 2 nodes of rotation and 2 nodes of the translational. The translation of the beam is free along the length direction of the beam and rotation is free around the axial axis of the roller support.

The model is loaded in the Y direction (Shown in Figure 5.9) by modifying the displacement on the sets of points as performed in Lab studies.

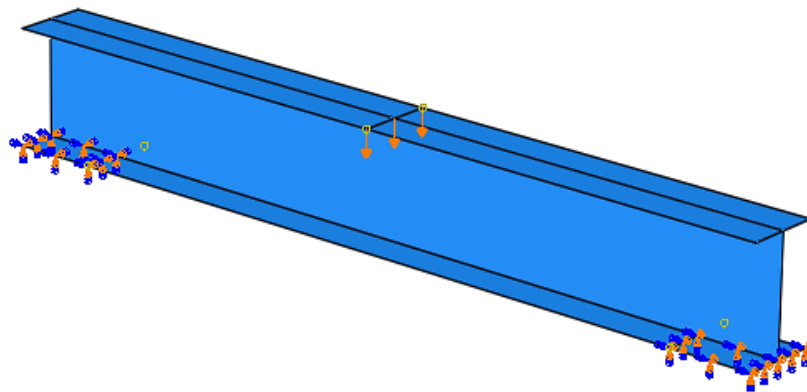


Figure 5.9. Boundary conditions of the model.

### 5.4. Geometry Imperfection

The responses of some structures are strongly depended on the imperfections in the original geometry, particularly if the buckling modes interact after buckling occurs. Thus, based on a single buckling mode imperfections tend to yield non-conservative results. The imperfection sensitivity of the structure can be assessed by adjusting the magnitude of the scaling factors of the various buckling modes.

Normally, the sensitivity of a structure to imperfections can be investigated by conducting a number of analyses. Structures with many closely spaced Eigen modes tend to be imperfection sensitive, and imperfections with shapes corresponding to the Eigen mode for the lowest eigenvalue may not give the worst case.

The analysis of the structure with the large imperfection is easy to analyze. The deformation will be quite small (relative to the imperfection) below the critical load, If the imperfection is small, Hence, the response will grow quickly near the critical load, introducing a rapid change in behavior. On the other hand, the post-buckling response will grow steadily before the critical load is reached if the imperfection is large. Thus, the transition into post-buckled behavior will be smooth and relatively easy to analyze in this case.

Imperfections are commonly provided by perturbations in the geometry. There are three ways offered by ABAQUS in order to define an imperfection: as a linear superposition of buckling Eigen modes, from the displacements of a static analysis, or by specifying the node number and imperfection values directly [56].

Different values of buckling Eigen modes have been considered as a trial in this study that had quite a small impact on the result and eventually the effect of imperfection has been ignored in the parametric study.

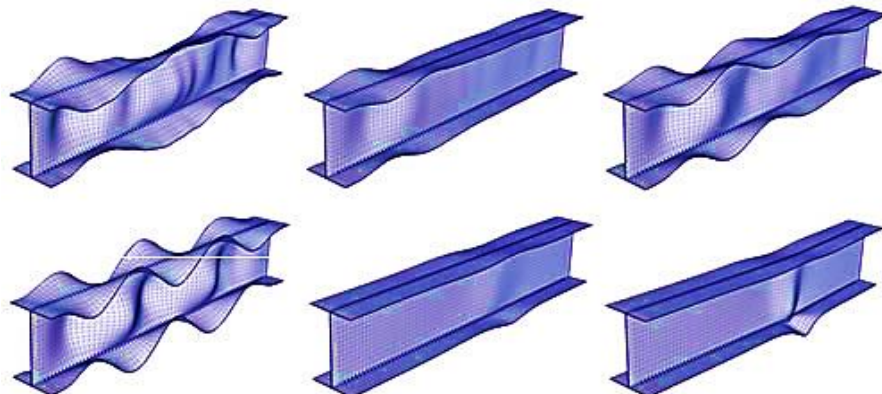


Figure 5.10. Buckling eigen value modes for imperfection [56].

## 5.5. Mesh

Meshing plays a very important role in the accuracy of the results in the Finite Element Analysis. Different type and size of the elements obtain different accuracy.

The model with intensive mesh sizes results accurately but it requires much more time which is better to select the optimum meshes. It is also not valid for an intensive mesh size to result more accurately; sometimes models are much more sensitive. The more important is the ratio between the dimensions of the elements [56].

The ratio between the dimensions of the elements in this model is relevantly taken constantly with the proportion of 1:1. Respectively 5X5 (M5), 10X10 (M10) and 15X15 (M15) meshing dimensions are provided to the model for trial purpose and hence the meshing with the dimensions of 10X10 (M10) is selected for being more accurate and efficient in the model analysis.

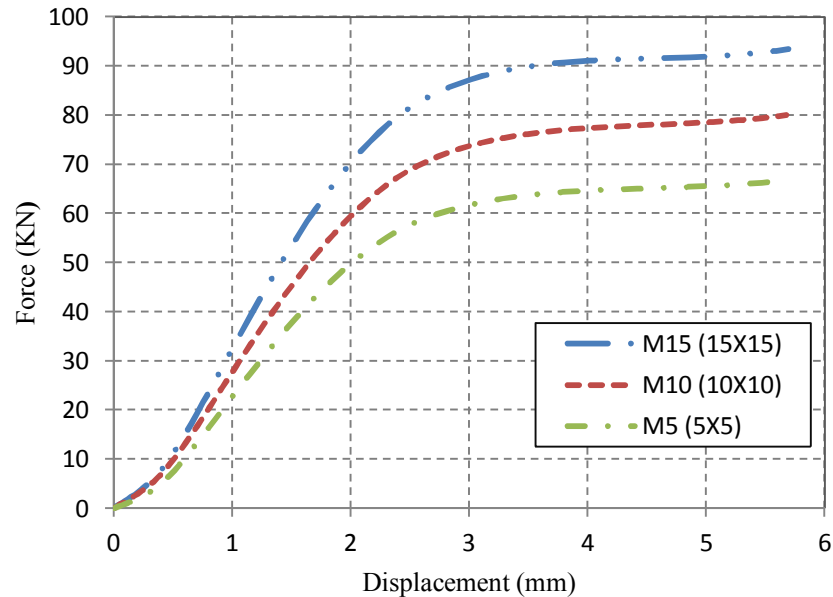


Figure 5.11. Meshing sensitivity of a model.

## 5.6. Fasteners

It is required to model the point to point connection between parts in some applications. These required connections may be from different types as spot welds, rivets, screws, bolts, or other types of fastening mechanisms. To provide bolt connection for the model, mesh-independent point fasteners are employed in the modeling. These connections can connect multiple layers and acts over a specified radius of influence. The fasteners are assumed to have the circular projection onto the connected surfaces [56].

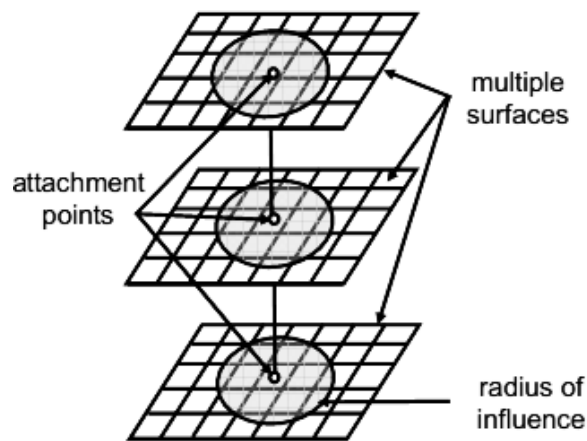


Figure 5.12. Mesh-independent point fasteners [56].

## 5.7. Model Verification

Considering the guidelines provided at the Documentation of ABAQUS and explanations stated in the above sections of Chapter 5, the models are created accordingly and eventually, the results received from the FEM analysis are checked against Lab studies for verification purpose.

The visualizations of stress on the surfaces of the FEM models (Reference Beam, CFRP retrofitted, CFRP retrofitted with bolt anchorage) under three point bending test are respectively shown in the Fig 5.13, Fig 5.14 and Fig 5.15.

The comparison for the both types of study (Lab and FEM) for each considered type of practice is represented in the form of graphs respectively in the Fig 5.16, Fig 5.17 and 5.18. The abbreviations as LAB, FEM, RB, HTCr and HTCbr respectively stand for Laboratory specimen, Finite Element Modal, Reference Beam, Heat Treated Beam with Carbon Retrofitting and Heated Treated Beam with Carbon & Bolt Retrofitting.

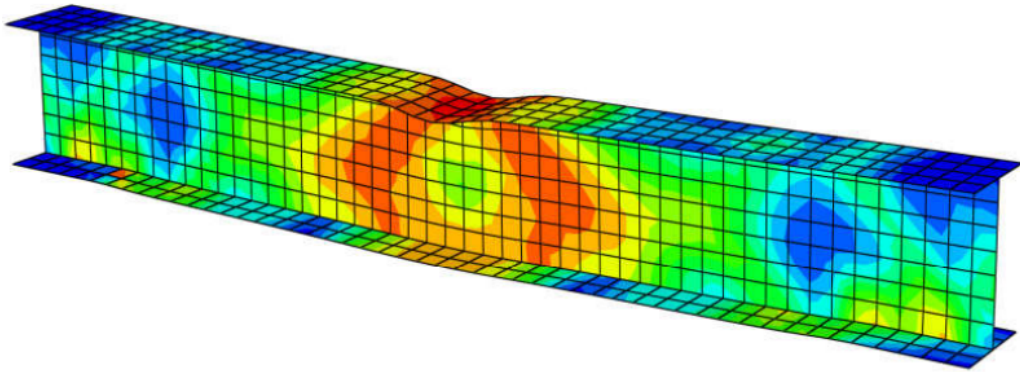


Figure 5.13. FEM IPE 80 RB.

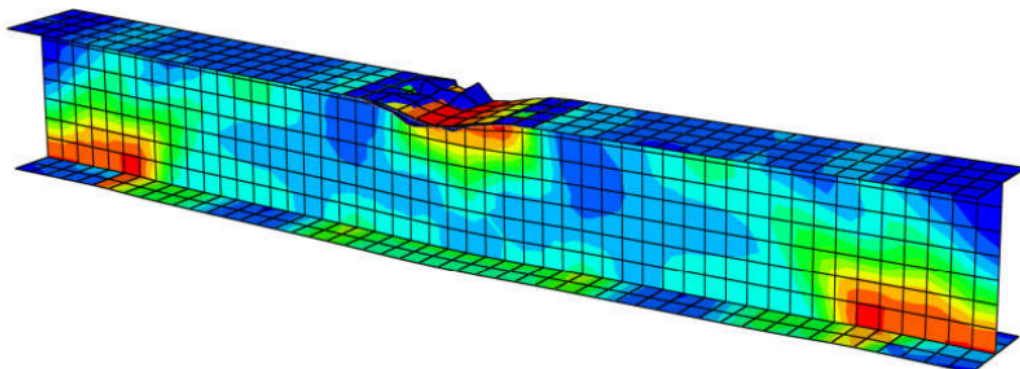


Figure 5.14. FEM IPE 80 HTCr.

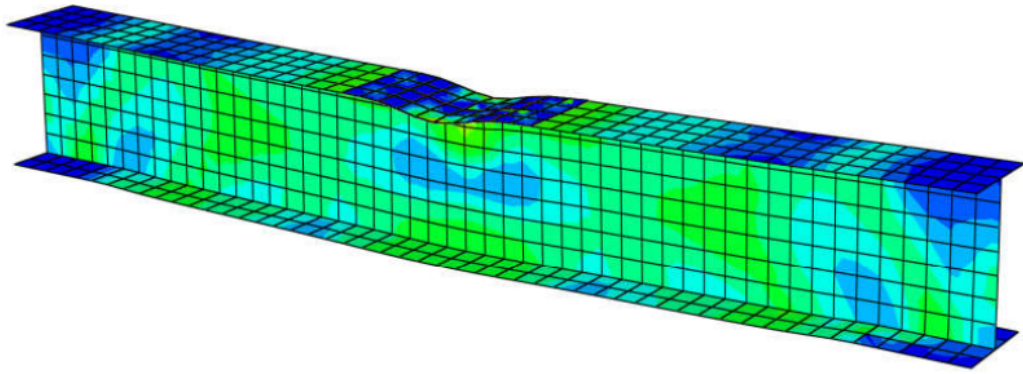


Figure 5.15. FEM IPE 80 HTCBr.

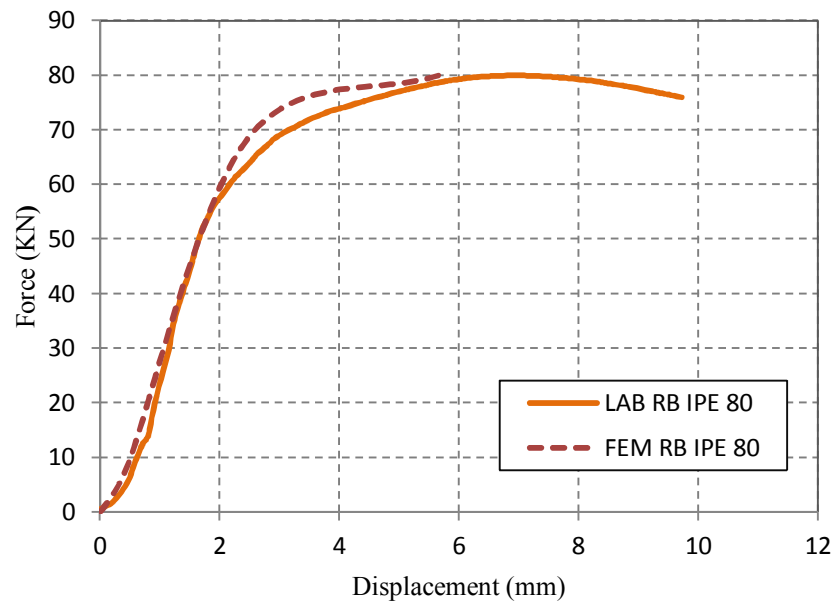


Figure 5.16. Force and displacement diagram (RB IPE 80).



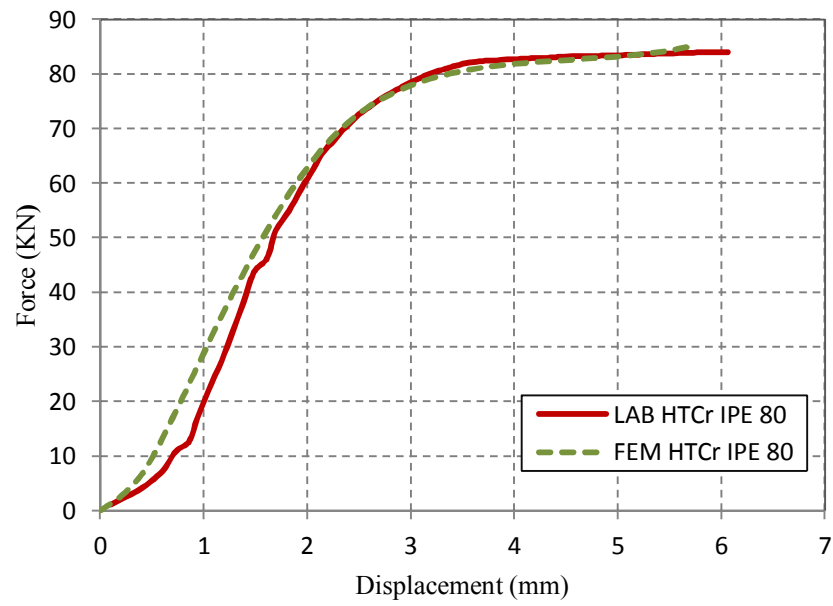


Figure 5.17. Force and displacement diagram (HTCr IPE 80).

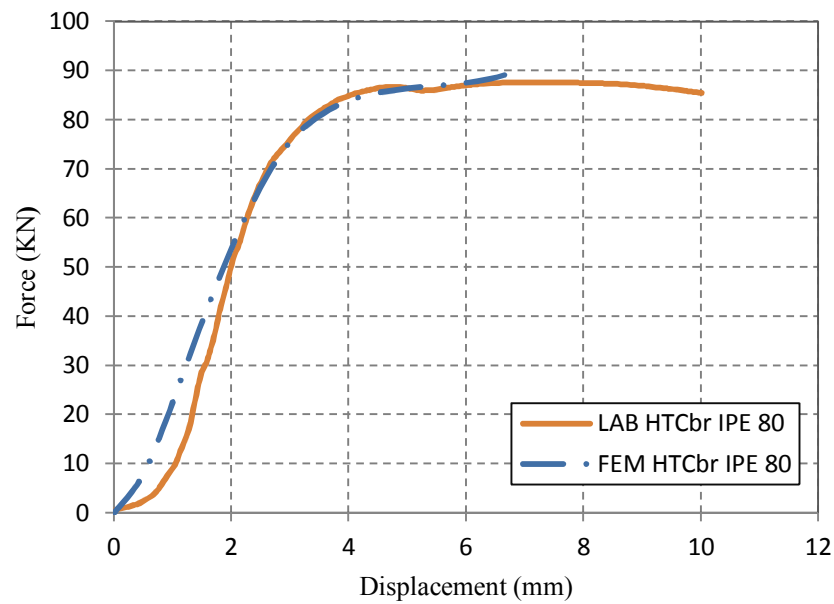


Figure 5.18. Force and displacement diagram (HTCbr IPE 80).

The comparison of the diagrams established from each type of FEM analysis and Lab experimental study comply with each other. The above graphs indicate the same behavior of elements resulted from FEM and Lab studies and have relatively close load capacity. Eventually; as the verification of the model is constructed, so it is

possible to produce a parametric study by using Finite Elements Models considering large-scale sections and spans.

## CHAPTER 6. PARAMETRIC STUDY

To observe the effect of CFRP on the heat-treated steel beams with the additional employment of bolts, it is required to investigate the mentioned practice on long and big sections. As it is not possible to implement the mentioned practice on real and actual beams due to non-existence and access to the devices with high capacities and dimensions, much more time-consuming, heavyweight and highly cost effect therefore FEM parametric study is most common in most academic studies, which are carried out after the validation of the model against the real lab specimen.

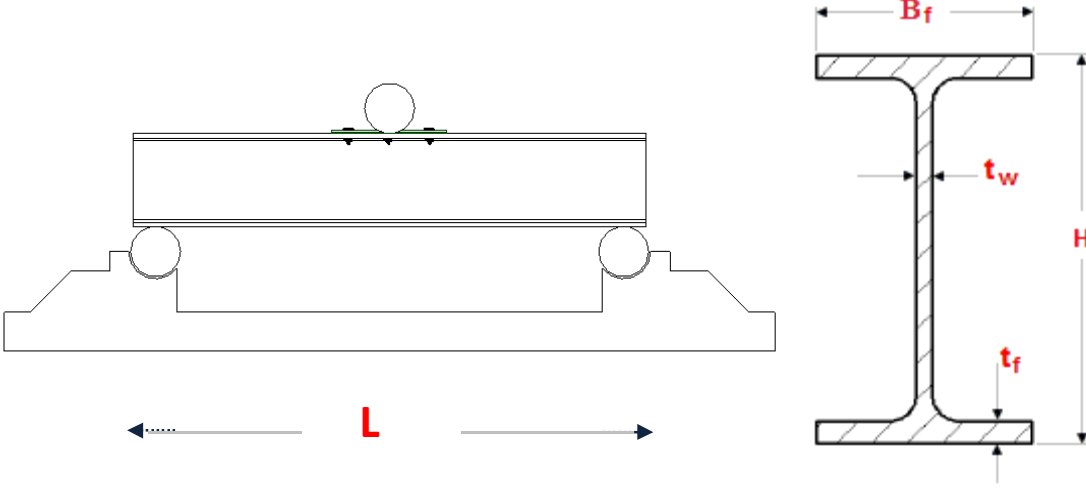
Variation of three physical quantities is considered in the present parametric investigation which is initially rooted from the flange slenderness ratio ( $B_f/2t_f$ ), the parameters are sub divided considering the web slenderness ratio ( $H/t_w$ ), and thus it is finally concluded with length to cross sectional depth ratio ( $L/B_f$ ). The parameters of each model are derived from the values gained from the above ratios. The dimensions of the height (H) and width ( $B_f$ ) for the entire models are considered constant which are respectively 600mm and 300 mm.

The study is carried out for the above models in a set of three groups, which are Reference specimens, CFRP retrofitted and CFRP retrofitted along with bolt employment ones.

In this study, the names of the models are abbreviated with some characters that respectively stands for, “RB” Reference Beam, “HT” Heat treated, “Cr” CFRP retrofitted, “HTCr” Heat treated CFRP retrofitted beam, “HTCBr” Heat treated CFRP retrofitted and bolt employed beam. 1, 2, 3, 4..... n indicates the number of the model in the parametric study.

A schematic description of this approach can be seen in Table 6.1. Cumulatively there will be at least 6 numbers of finite elements runs for each  $B_f/t_f$  group set which totally makes 36 numbers of finite element runs in the entire study.

Table 6.1. Parameters of the specimens for parametric study



Model	$B_f/t_f$	$H/t_w$	$L/B_f$	$L/H$	H	$B_f$	$t_f$	$t_w$	L
1	11	109	8	4	600	300	27.3	5.5	2400
2			12	6	600	300	27.3	5.5	3600
3			16	8	600	300	27.3	5.5	4800
4		165	8	4	600	300	27.3	3.6	2400
5			12	6	600	300	27.3	3.6	3600
6			16	8	600	300	27.3	3.6	4800
7	30	109	8	4	600	300	10	5.5	2400
8			12	6	600	300	10	5.5	3600
9			16	8	600	300	10	5.5	4800
10		165	8	4	600	300	10	3.6	2400
11			12	6	600	300	10	3.6	3600
12			16	8	600	300	10	3.6	4800

The values  $B_f/2t_f$  and  $H/t_w$  are derived from AISC – Table B4.1 of compact and non-compact sections for the A36 type of steel.

### 6.1. FEM Experimental Results

The results established from the FEM analysis of beam models described above in Table 6.1 are shown in the following diagrams. The FEM analysis for each type of study (Reference, CFRP retrofitting and Mechanical anchorage retrofitting) of each model are carried out and their graphs are relatively represented together for comparison.

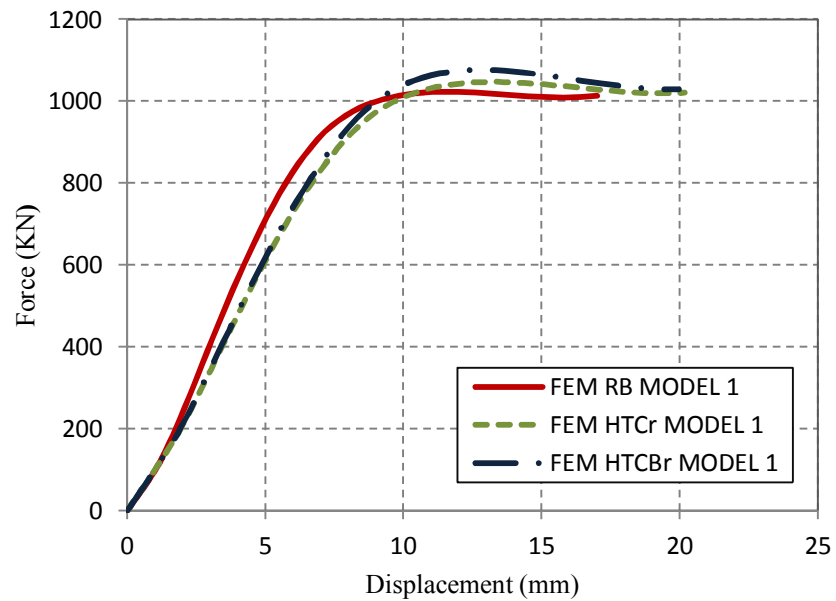


Figure 6.1. Force and displacement diagram (MODEL 1).

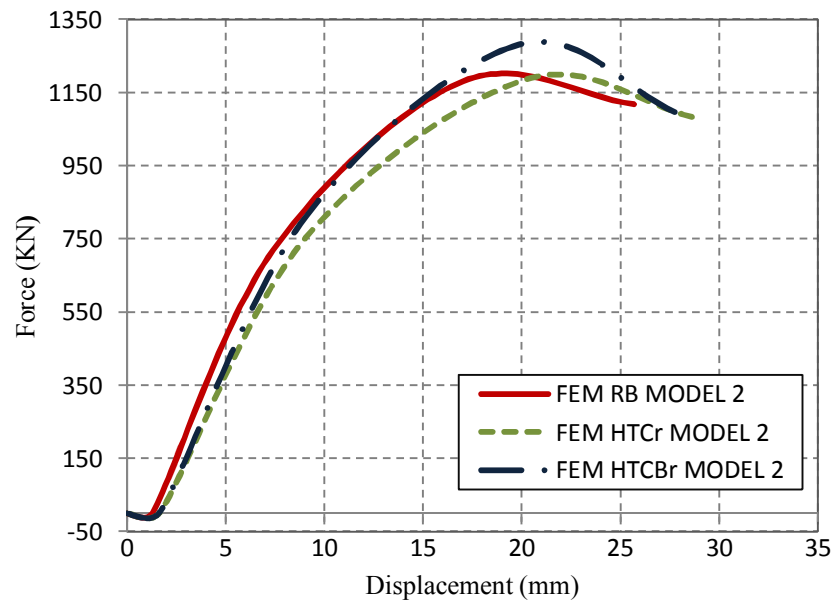


Figure 6.2. Force and displacement diagram (MODEL 2).

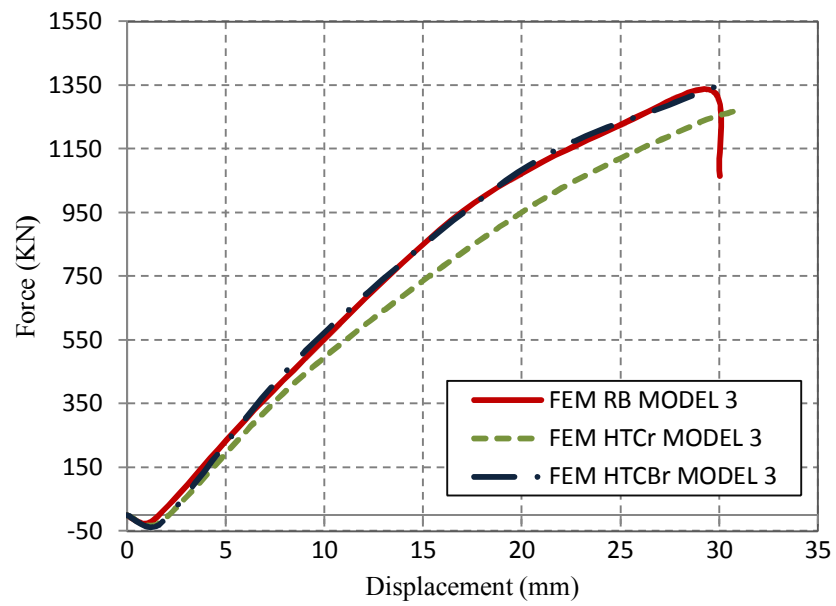


Figure 6.3. Force and displacement diagram (MODEL 3).

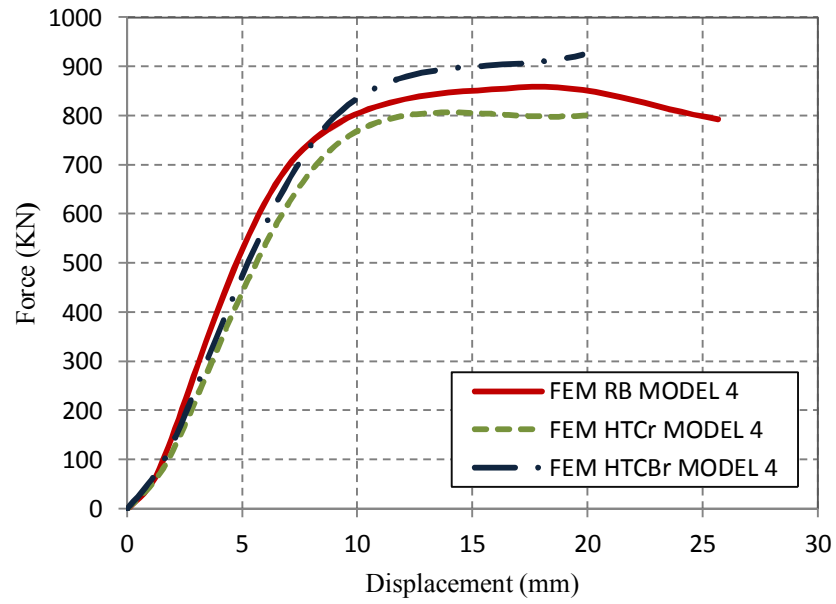


Figure 6.4. Force and displacement diagram (MODEL 4).

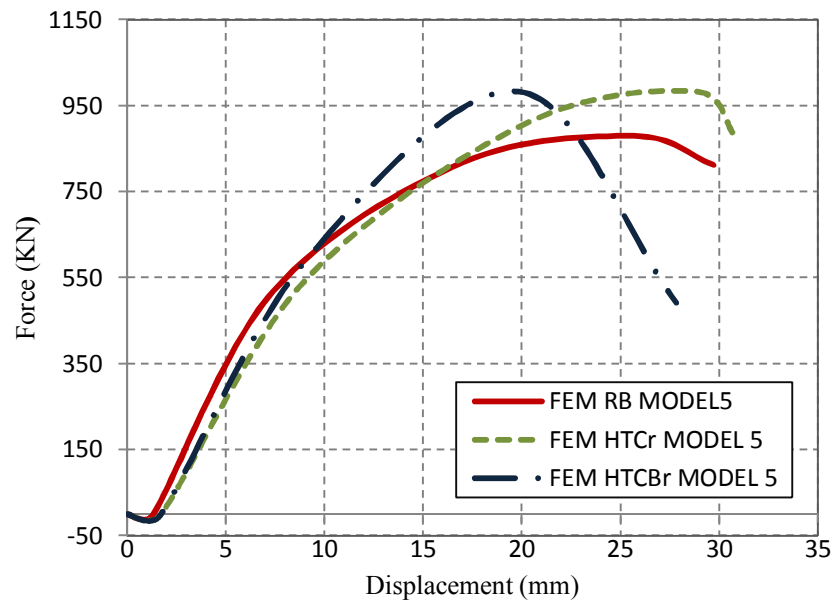


Figure 6.5. Force and displacement diagram (MODEL 5).

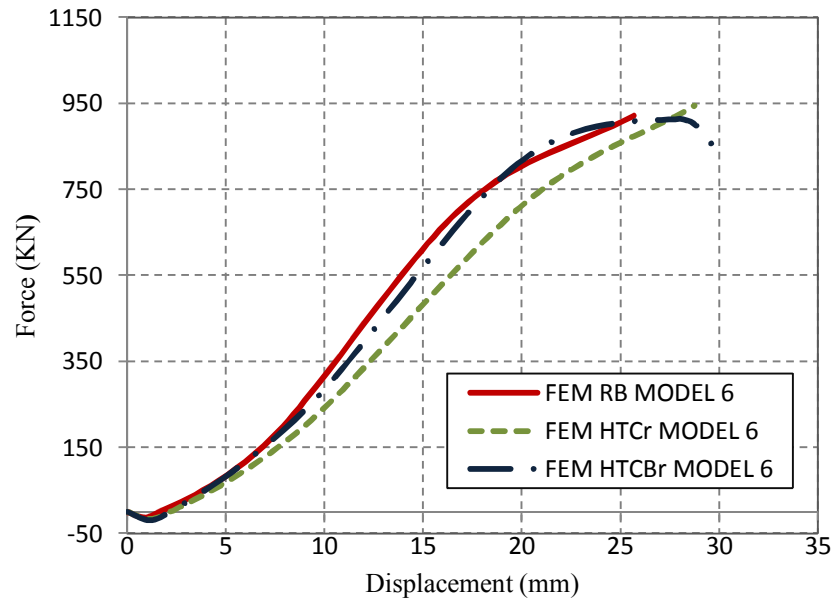


Figure 6.6. Force and displacement diagram (MODEL 6).

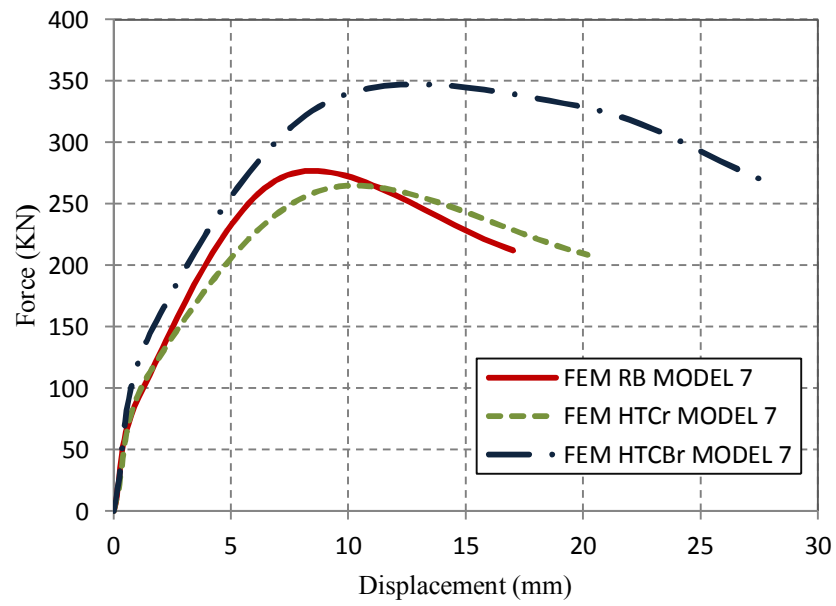


Figure 6.7. Force and displacement diagram (MODEL 7).



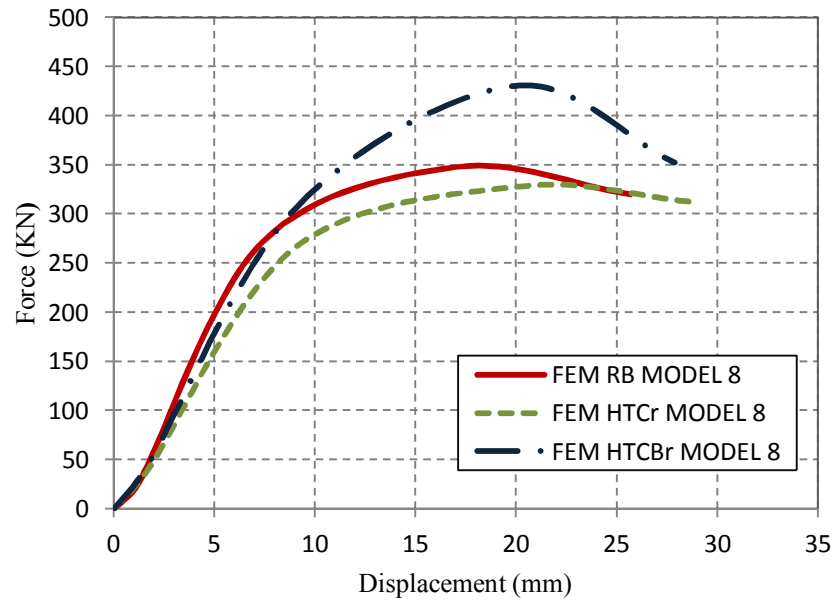


Figure 6.8. Force and displacement diagram (MODEL 8).

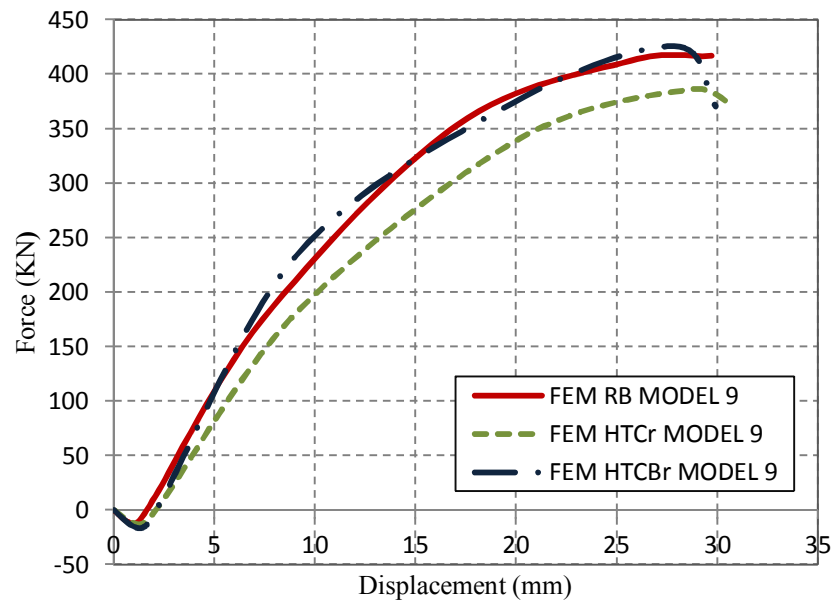


Figure 6.9. Force and displacement diagram (MODEL 9).

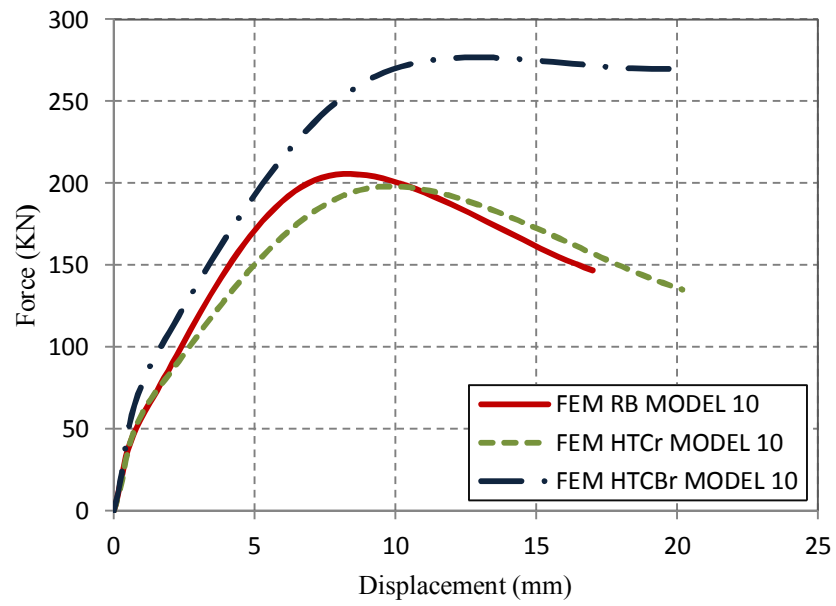


Figure 6.10. Force and displacement diagram (MODEL 10).

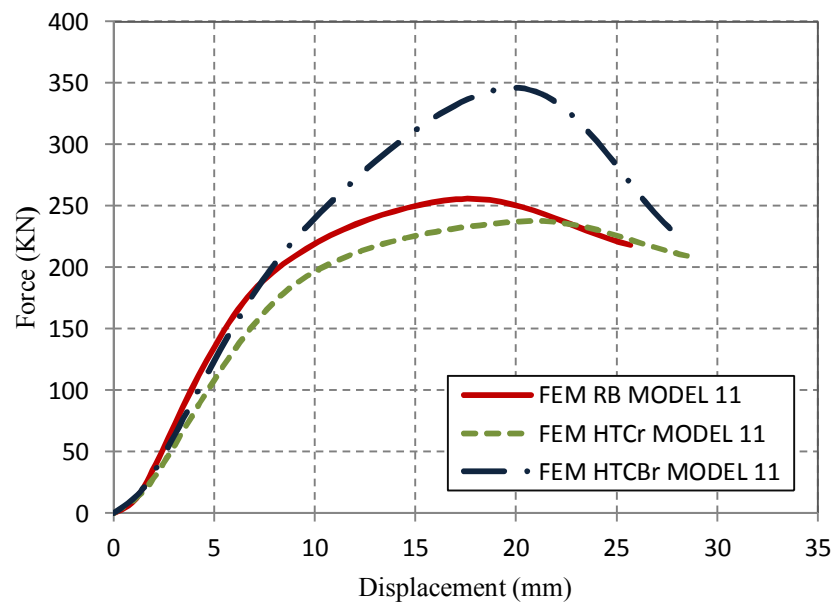


Figure 6.11. Force and displacement diagram (MODEL 11).

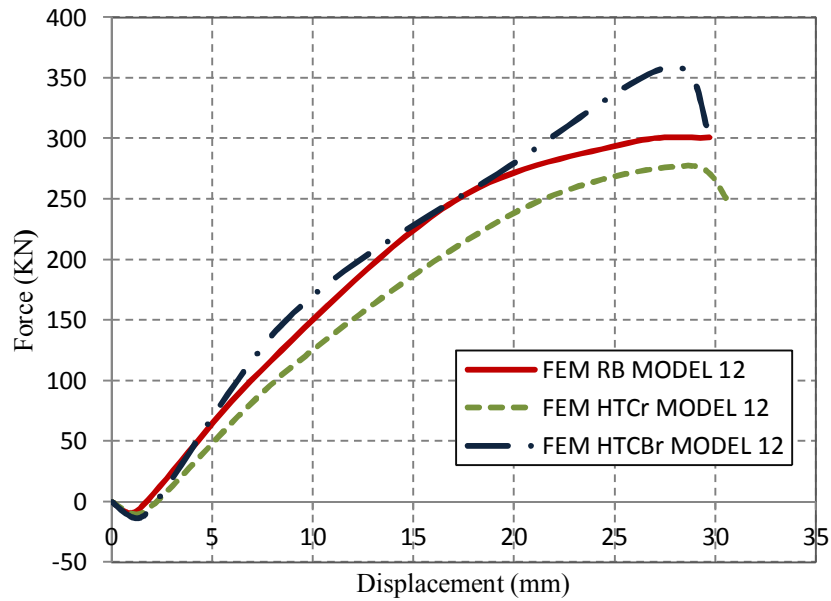


Figure 6.12. Force and displacement diagram (MODEL 12).

In order to determine the effect of Mechanical Anchorage in Compact and Non-Compact beams (Refer to Table 6.1), the results gained from FEM analysis of the Reference and HTCBr ones are compared as shown in Table 6.2 and Figure 6.13.

Table 6.2. Comparison of FEM reference beams against mechanically retrofitted beams

Set	MODELS	FEM Experimental Results			
		Reference Beam	Mechanical Anchorage		Remarks
		Max Load (KN)	Max. Load (KN)	Load Difference %	
A	1	1013	1124	10.95	Increase
	2	1181	1281	8.47	Increase
	3	1330	1345	1.12	Increase
	4	857	924	7.81	Increase
B	5	879	983	11.83	Increase
	6	913	924	1.2	Increase
	7	273	332	21.6	Increase
C	8	347	430	23.9	Increase
	9	412	425	3.15	Increase
	10	203	269	32.5	Increase
D	11	255	346	35.6	Increase
	12	300	359	19.6	Increase

The Models considered under Set A and B are compact sections, since the flange slenderness ratio ( $B/t_f$ ) of the sections are sufficiently small and the flange

slenderness ratio ( $B/t_f$ ) of the Models considered under Set C and D are larger which is classified as Non Compact Sections (Refer to Table 6.1).

The web Slenderness ratio ( $H/t_w$ ) respectively of Set A & C and Set B & D are same (Refer to Table 6.1), both of which varies from each other (Set A & C compare to Set B & D).

Considering the parameters of the examined FEM Models against the results derived from FEM analysis, it is observed that employment of the bolt anchorage increases the load capacity of the heat treated elements and sustains the elements to resist more loads. However the behavior and strengthening capacity of this practice is accordingly dependent on the flange slenderness ratio ( $B/t_f$ ) and web Slenderness ratio ( $H/t_w$ ) of the proposed beam.

For better understanding and more elaboration, the percentage of the load capacity of the examined FEM models due to the employment of mechanical anchorage is comparatively represented in the Fig. 6.13.

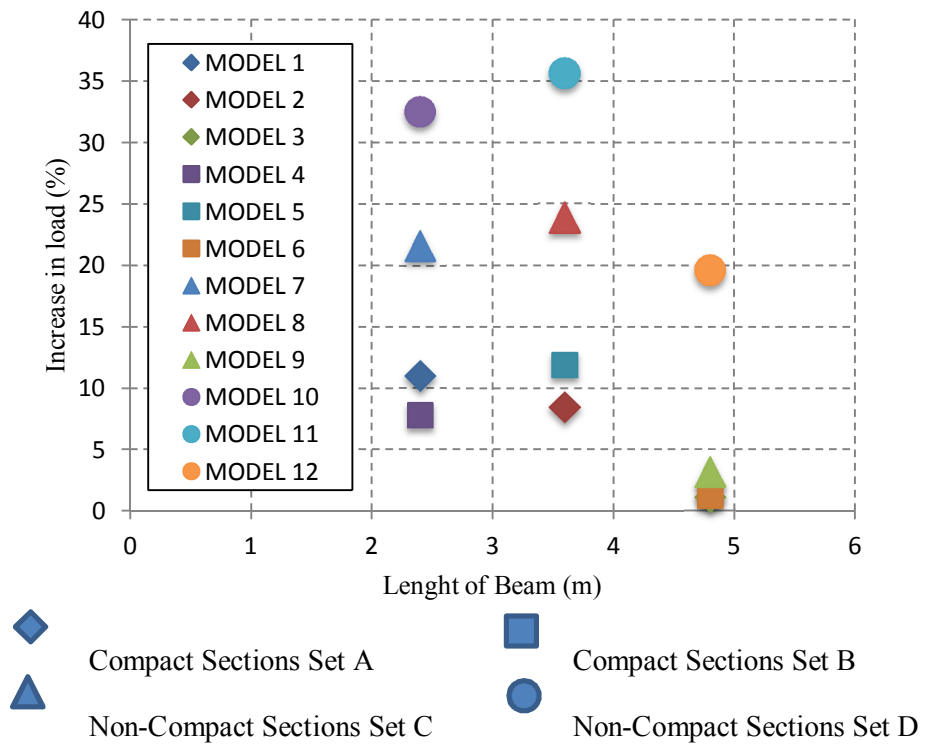


Figure 6.13. Effect of mechanical anchorage in compact and non-compact sections.

## CHAPTER 7. RESULTS AND RECOMMENDATIONS

It has been observed from the Lab and FEM analysis that employing bolt anchorage along with epoxy bonding to the heat-treated areas of a deformed specimen causes the element to resist much more load and shows a good behavior compare to its other counterparts. However, implementation of this practice is a little bit complicated compared to only CFRP and epoxy bonding but it's much more satisfactory.

It has also been noticed that the result of mechanical anchorage practice is accordingly proportional to flange slenderness ratio ( $B/t_f$ ), web Slenderness ratio ( $H/t_w$ ) and the length of the proposed beam. The results derived from FEM parametric studies indicate that the efficiency of mechanical anchorage in short span beams is higher compared to the long span beams. Simultaneously the behavior of compact and non-compact sections has additional influence on the same considered length of the specimens.

The results of the FEM parametric study could be concluded as follow:

- a. The Models under Set A (1, 2 & 3) and Set B (4, 5 & 6) has respectively same span of 2400, 3600 and 4800 mm length, both of which are compact sections but the web slenderness ratio ( $H/t_w$ ) of Set B is higher than Set A. The result reveals that the FEM HTCBr Models under Set B (4, 5 & 6) has increased the capacity of their related Reference beams respectively 3.14%, 3.36% and 0.08% more than the FEM HTCBr Models under Set A (1, 2 & 3).
- b. The Models under Set C (7, 8 & 9) and Set D (10, 11 & 12) has respectively same span of 2400, 3600 and 4800 mm length, both of which are noncompact sections but the web slenderness ratio ( $H/t_w$ ) of Set D is higher than Set C. The result

reveals that the FEM HTCBr Models under Set D (10, 11 & 12) has increased the capacity of their related Reference beams respectively 10.9%, 11.7% and 16.45% more than the FEM HTCBr Models under Set C (7, 8 & 9).

- c. Model 10 which is short span non-compact section with the highest web slenderness ratio has mostly increased the load capacity of its related Reference beam (32.5 %) compare to Model 7 a non-compact section with small web slenderness ration (21.6%), Model 4 a compact section with high web slenderness ratio (7.81%) and Model 1 a compact section with small web slenderness ratio (7.81%). All these models have the same length of 2400 mm.
- d. Model 11 which is medium span non-compact section with the highest web slenderness ratio has mostly increased the load capacity of its related Reference beam (35.6 %) compare to Model 8 a non-compact section with small web slenderness ration (23.9%), Model 5 a compact section with high web slenderness ratio (11.83%) and Model 2 a compact section with small web slenderness ratio (8.47 %). All these models have the same length of 3600 mm.
- e. Model 12 which is long span non-compact section with the highest web slenderness ratio has mostly increased the load capacity of its related Reference beam (19.6 %) compare to Model 9 a non-compact section with small web slenderness ration (3.15 %), Model 6 a compact section with high web slenderness ratio (1.2 %) and Model 3 a compact section with small web slenderness ratio (1.12 %). All these models have the same length of 4800 mm.
- f. The medium and short span Models under each Set (short, medium, long) has respectively higher percentage figure of capacity increase compare to long span Model. Set A (10.95 %, 8.47 % & 1.12 %), Set B (7.81 %, 11.83 % & 1.2 %), Set C (21.6 %, 23.9 % & 3.15 %) and Set D (32.5 %, 35.6 % & 19.6 %).

Eventually; employing mechanical anchorage on CFRP plates with epoxy bonding to the heat treated areas of beams are much more effective and significantly develops the strength of the beam, especially in the noncompact sections with higher web slenderness ratio having short or medium spans.

The parametric study does also reveal that bonding the CFRP plates by epoxy to the faces of the heat treated areas without any mechanical anchorage may not cause effectively in order to develop the strength of the heat treated areas, since existence of load at the retrofitted area will lead epoxy to scatter rapidly, which results an early traction and separation of CFRP plates from the bonded area of steel element.

This study is carried out through scaled specimens considering three-point bending test and hereby it is suggested that this practice should be developed on real beams, girders or FEM analysis for further observations though four-point bending test which will give much more real and accurate results, furthermore the effect of mechanical anchorage on the long span beams under four-point bending test shall be investigated for better observations.



## REFERENCES

- [1] Wang, C.M., Wang, C.Y., Reddy, J.N., Exact solutions for buckling of structural members, CRC Press, ISBN 0-8493-2222-7, 2005.
- [2] Rail Corp engineering manual, TMC 302, Structures repair, Version 2.0, 2009.
- [3] Alberta transportation, Repair of bridge structural steel elements manual, Version 1.0, 2004.
- [4] Aydin, Emine., Aktas, Muhheram., Obtaining a permanent repair by using GFRP in steel plates reformed by heat-treatment, Thin-Walled Structures 94 (2015) 13–22, 2015.
- [5] Mallick, P.K., Fiber-reinforced composites materials, manufacturing and design, CRC press, ISBN 13: 978-0-8493-4205-9, 2007.
- [6] Demir, Hasan., Strengthening, and repair of steel bridges-Techniques and management, Master's Thesis 2011:139, Department of Structural Engineering, Chalmers University of Technology, Göteborg, Sweden,2011.
- [7] Cuevas, Sherron., Fiber materials and Technology, First edition, Library Press, ISBN 978-81-323-2187-3, 2012.
- [8] Lackowski, Matthew., Varma, Amit., Heat Treatment and Its Effects on Rehabilitating Steel Bridges in Indiana, Purdue University, FHWA/IN/JTRP-2007/3.
- [9] Holloway, L.C., The evolution of and the way forward for advanced polymer composites in the civil infrastructure, Construct. Build. Mater., 17:365 (2003).
- [10] Haghani, R., Behavior and design of adhesive joints in flexural steel members bonded with FRP laminates, Ph.D. Thesis, Department of Structural Engineering, Chalmers University of Technology, Gothenburg, Sweden, pp 1-24, 2010.

- [11] Tilly, G.P., Matthews, S.J., Deacon, D., De Voy, J., Jackson, P.A., Iron and steel bridges: condition appraisal and remedial treatment, CIRIA, London, 2008.
- [12] Cadei, J.M.C., Stratfoed, T.J., Hollaway, L.C., Duckett, W.G., Strengthening metallic structures using externally bonded fiber reinforces polymers, CIRIA, London.PP1-49, 2004.
- [13] Test resources Inc., Bend flexure test., [www.testresources.com](http://www.testresources.com)., Access Date: 20.04.2016.
- [14] [www.reddit.com/.](http://www.reddit.com/), Access Date: 15.03.2016.
- [15] Admet., Materials testing system manufacturer., [www.admet.com](http://www.admet.com)., Access Date: 15.03.2016.
- [16] Hirohata, M., Kim, Y.C., Dominant factors deciding compressive behavior of cruciform column projection panel corrected by heating, Steel Structures 7, 193-199, 2007.
- [17] Hirohata, M., Kim, Y.C., Generality verification for factors dominating mechanical behavior under compressive loads of steel structural members corrected by heating/pressing, Steel Structures 8, 83-90, 2008.
- [18] Alsayed, S.H., Al-salloum, Y.A., Almusallam, T.H., Fibre-reinforced polymer repair materials-some facts. Proceedings of the Institution of Civil Engineers, Civil Engineering 2000;138(3), 131–4, 2000.
- [19] Moy, S., Ice., Design and Practice Guides-FRP composites life extension and strengthening of metallic structures. London (UK): Thomas Telford Publishing, 2001.
- [20] Teng, J.G., Chen, J.F., Smith, S.T., Lam, L., FRP-strengthened RC structures, West Sussex (UK): John Wiley and Sons Ltd, 2002.
- [21] Tavakkolizadeh, M., Saadatmanesh, H., Strengthening of steel-concrete composite girders using carbon fibre reinforced polymer sheets, Journal of Structural Engineering, ASCE 2003;129(1), 30–40, 2003.
- [22] Jones, S.C., Civjan, S.A., Application of fibre reinforced polymer overlays to extend steel fatigue life, Journal of Composites for Construction, ASCE 2003;7(4), 331–338, 2003.
- [23] Schnerch, D., Stanford, K., Lanier, B., Rizkalla, S., Use of high modulus carbon fibre reinforced polymer (CFRP) for strengthening steel structures, In:

2nd Int. Workshop On Structural Composites For Infrastructure Applications, 2003.

- [24] Chacon, A., Chajes, M., Swinehart, M., Richardson, D., Wenczel, G., Application of advanced composites to steel bridges: A case study on the Ashland bridge (Delaware-USA), *Advanced Composite Materials In Bridges And Structures*, 2004.
- [25] Mosallam, A.S., Composites: Construction materials for the new era, *Advanced Polymer Composites for Structural Applications In Construction*, 45–58, 2004.
- [26] Nikouka, F., Lee, M., Moy, S., Strengthening of metallic structures using carbon fibre composites, *IABSE (International Association for Bridge and Structural Engineering) Symposium 2002*, 2002.
- [27] Hollaway, L.C., Cadei, J., Progress in the technique of upgrading metallic structures with advanced polymer composites, *Progress in Structural Engineering and Materials* 2002;4(2), 131–148, 2002.
- [28] Cadei, J.M.C., Stratford, T.J., Hollaway, L.C., Duckett, W.G., *C595-Strengthening metallic structures using externally bonded fibre-reinforced composites*, London: CIRIA, 2004.
- [29] Luke, S., Canning, L., Strengthening highway and railway bridge structures with FRP composites-Case studies, *Advanced Polymer Composites For Structural Applications In Construction*, 747–754, 2004.
- [30] Suzuki, H., First application of carbon Fiber reinforced polymer strips to an existing steel bridge in Japan, *Advanced materials for construction of bridges, buildings and other structures*, 2005.
- [31] Bassetti, A., Nussbaumer, A., Hirt, M.A., Crack repair and fatigue extension of riveted bridge members using composite materials, *Bridge engineering conference, ESE-IABSE-FIB*, 227–238, 2000.
- [32] Ağcakoca, E., I-kesitli çelik-betonarme kompozit kirişlerin HM-CFRP ile onarım ve güçlendirilmesine yönelik metot geliştirilmesi, *Sakarya Üniversitesi, Doktora Tezi*, 2012.
- [33] Sayed-Ahmed, E.Y., Strengthening of thin-walled steel I-section beams using CFRP strips, *Proceedings of the 4th International Conference on Advanced Composite Materials in Bridges and Structures*, Calgary, July 2004.

- [34] Sen, R., Liby, L., Mullins, G., Strengthening steel bridge sections using CFRP laminates, *Composites Part B*. 32, 309-322, 2001.
- [35] Chiew, S.P., Lie, S.T., Lee, C.K., Yu, Y., Debonding failure model for FRP retrofitted steel beams, *Advances in Steel Structures* 1, 579 -586, 2005.
- [36] Colombi, P., Poggi, C., An experimental, analytical and numerical study of the static behavior of steel beams reinforced by pultruded CFRP strips, *Composites: Part B* 37, 64–73, 2006.
- [37] Colombi, P., Fava, G., Fatigue crack growth in steel beams strengthened by CFRP strips, *Theoretical and Applied Fracture Mechanics*, 2016.
- [38] El Damatty, A.A., Abushagur, M., Youssef, M.A., Rehabilitation of composite steel bridges using GFRP plates, *Applied Composite Materials* 12, 309 – 325, 2005.
- [39] Accord, N. B., Earls, C. J., Use of fiber reinforced polymer composite elements to enhance structural steel member ductility, *Journal of Composites for Construction ASCE* 10.4, 337-344, 2006.
- [40] Patnaik, A.K., Bauer, C.L., Strengthening of steel beams with carbon FRP laminates, *Proceedings of the 4<sup>th</sup> International Conference on Advanced Composite Materials in Bridges and Structures*, Calgary, July 2004.
- [41] A.H, Alsaïdy., Klaiber, F.W., Wipf, T.J., Strengthening of steel concrete composite girders using carbon fiber reinforced polymer plates, *Construction and building materials*, 1122-1135, 2009.
- [42] Fam, Amir., Macdougall, Colin., Shaat, Amr., Upgrading steel–concrete composite girders and repair of damaged steel beams using bonded CFRP laminates, *Thin-Walled Structures*, 47 (2009).
- [43] Sweedan, Amr M.I., Alhadid, Mohammed M.A, El-Sawy, Khaled M., Experimental study of the flexural response of steel beams strengthened with anchored hybrid composites, *Thin-Walled Structures*, 99 (2016) 1-11, 2016.
- [44] Kim, Hee Sun., Shin, Yeong Soo., Flexural behavior of reinforced concrete (RC) beams retrofitted with hybrid fiber reinforced polymers (FRPs) under sustaining loads, *Composite Structures* 93 (2011) 802–811, 2011.
- [45] ASTM A370-10, Standard test methods and definitions for mechanical testing of steel products, ASTM (American Society for Testing and Materials), 2010.

- [46] Sika Yapı Kimyasalları A.Ş, 2012.
- [47] ASTM D 3039 M-08, Standard test method for tensile properties of polymer matrix composite materials, ASTM (American Society for Testing and Materials), 2007.
- [48] TS EN ISO 527-4 Plastikler- çekme özelliklerinin tayini- Bölüm 4: İzotropik ve ortotropik elyaf takviyeli plastik kompozitler için deney şartları, Türk Standartları Enstitüsü, 2007.
- [49] TS EN ISO 527-5 Plastikler- Çekme özelliklerinin tayini- Bölüm 5: Tek yönlü elyaf takviyeli plastik kompozitler için deney şartları, Türk Standartları Enstitüsü, 2010.
- [50] Adams, Daniel O., Adams, Donal F., DOT/FAA/AR-02/106, Tabbng Guide for composite test specimen, Department of Mechanical Engineering, University of Utah, Salt Lake City, 2002.
- [51] European standard profile sections catalogue.
- [52] Alşa laboratuvar cihazları., Hidrolik universal test cihazları., [www.alsalab.com](http://www.alsalab.com)., Access Date: 20.04.2016.
- [53] Autograph AG-IC series, Shimadzu Precision universal tester, catalogue.
- [54] Optimum, Metal working machines, catalogue.
- [55] Dere Yaman, Z., Mercan Eryılmaz, D., Aktas, M., Elmas, M., Doğrusal olmayan sonlu elemanlar analizinde çelik eğilme elemanlarının geometrik kusurlarının tanımlanması, Türkiye Abaqus Kullanıcıları Toplantısı, 215-222, 2010.
- [56] ABAQUS/Standard User's Manual, Version 6.11. Hibbitt, Karlson& Sorensen, Inc, Pawtucket, RI, 2011.
- [57] Hibbeler, R.C., Mechanics of Materials, 8th Edition, Pearson Prentice Hall, ISBN 13: 978-0-13-602230-5, 2011.

## **RESUME**

Abdul Majeed Qarizada born on 26 October 1989 at Laghman Afghanistan is young professional Engineer who has completed his Secondary and High School educations at Nangarhar High School, Nangarhar in 2006. Passing the University Entry Test Exam with high marks, Qarizada started Civil Engineering at Nangarhar University, Nangarhar with an extreme ambition, who has successfully completed his B.Sc. degree gaining top rank marks. Qarizada with his multi-language speaking talent is currently holding Turkish Scholarship to complete his M.Sc. studies in Civil Engineering at the Sakarya University, Sakarya.